NEW SEISMIC DEPTH PROFILES ON TAKU GLACIER - 1993

Juneau Icefield, Alaska

Geophysical Team

Maynard M. Miller (project leader)
Timothy D. Benedict (compiler)
Kenneth F. Sprenke (technical adviser)
Geoff E. Gilbert (field assistant)
Jamie R. Stirling (field assistant)

OPEN FILE REPORT - JIRP 1993

Glaciological and Arctic Sciences Institute
University of Idaho
Moscow, Idaho 83844

1993

Abstract

During the field season of 1993, seismic investigations were carried out on the Juneau Icefield, Alaska, under the auspices of the Foundation for Glacier and Environmental Research. The seismic study revealed depths of 500-800m for the upper Matthes Glacier, 400-500m for the Vaughan Lewis Glacier, 600-700m for the Matthes-Llewellyn divide, and under 400m for the Bücher Glacier. In all 1993 seismic work the Poulter Method of using above-surface explosions was found to be the most effective technique for producing clear seismic records. Furthermore, research in conjunction with radio-echo sounding techniques was done to determine a P-wave velocity in ice of 3660 m/s.

Introduction

Two widely employed geophysical techniques for constructing glacier depth profiles include radio-echo sounding and seismic methods. Radio-echo sounding is the most popular technique in current glaciological research, and it has been used extensively in Antarctica and other regions with polar and sub-polar ice. However, radio-echo sounding (radar) performs inconsistently on temperate glaciers because of their high water content (Paterson 1981). On the other hand, seismic methods, although cumbersome and somewhat old-fashioned, are not greatly dependent on glacier water content and therefore can be employed on a polar or temperate glacier equally well. Many workers have used seismic techniques in glacier depth surveys, and some of the major studies include Hobson and Jobin in British Columbia (1975), Röthlisberger on Baffin Island (1955), Allen and Smith in Alaska (1953), Robin in Antarctica (1952), and Doell in British Columbia (1963).

On the Juneau Icefield, which is a temperate glacier system, seismic surveying has been the method of choice for obtaining depth profiles, and since the mid-1940's three main seismic surveys have been carried out. The first was done by Poulter in 1949, followed by Senstad and Rifkind in 1983 and Nolan in 1992. However, these surveys did not produce consistent results, and there is a particularly great discrepancy between Poulter and Nolan, as Nolan's glacier depths in some instances are almost 400% greater than Poulter's.

The primary goal of the geophysical work on the Juneau Icefield during the field season of 1993 was to end the confusion rising from the inconsistency between the earlier studies by completing seismic surveys on several major glaciers. Furthermore, the excellent summer weather allowed the geophysical survey to explore other profile techniques such as radar and gravity methods. Radar, although ill-suited to the temperate ice, showed promise and complemented the seismic survey in some instances. Its specific results will be reported elsewhere. The gravity work also evolved into its own separate survey and will be reported in another paper.

Physical Setting of the Juneau Icefield

The Juneau Icefield, which is located in southeast Alaska and northwest British Columbia, is a relict of the Cordilleran ice sheet (Marston 1983). Its southwestern edge is about 10-15 km from the Alaskan capital city of Juneau, and the ice extends northeast across the U.S./Canadian border, almost reaching Atlin Lake in British Columbia (Figure 1). The most significant glacier in the icefield, the Taku Glacier, extends approximately 45-50 km from Névé to terminus. Other major glaciers include the Herbert and Mendenhall glaciers on the icefield's western edge, the Matthes and Demorest glaciers in the central portion of the icefield, and the Llewellyn Glacier which reaches toward Atlin in the northeast.

The Juneau Icefield is significant because it is representative of the glaciated region in southeast Alaska, which contains the world's largest area of concentrated glacial ice outside of the high Arctic and the Antarctic. However, unlike most of southwest Alaska, the Juneau Icefield is in a region of relative tectonic stability, which implies that glacier behavior observed there is primarily controlled by climatic and not tectonic factors (Miller 1985). Therefore the icefield is an excellent prototype region for the study of climatic change, which in turn has great practical implications for research on global warming and the greenhouse effect. This naturally underlines the importance of knowing the basic physical parameters of the glaciers of the icefield - particularly their depth profiles - as these are foundational for climate study or any other interdisciplinary work

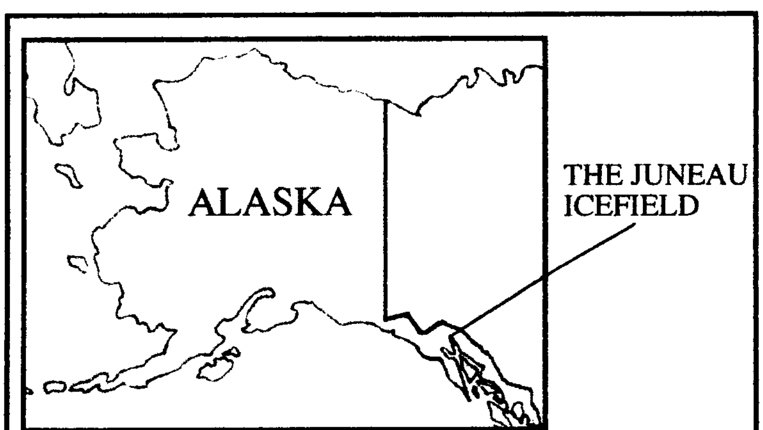

FIGURE ONE

Research on the Juneau Icefield is primarily carried out by the Juneau Icefield Research Program (JIRP) which was organized in 1946 under the direction of Dr. Maynard M. Miller. Since then JIRP has carried out research on the Juneau Icefield in many glaciological disciplines, including glacier deformation experiments, glaciothermal studies, and glacio-hydrology in addition to work in bedrock geology, general geomorphology, and ecology. All of the members of the 1993 seismic survey were members of JIRP, and all equipment and logistics were provided by JIRP as well.

Location of Seismic Profiles on the Juneau Icefield

Seismic soundings were carried out on six previously established survey profiles on four glaciers in the Juneau Icefield (Figure 2). Profile IV was done on July 20-25 on a transect of the Taku Glacier between Camp 10 ("Nunatak Chalet" on USGS maps) and Shoehorn Mountain. Profile II was carried out on the Taku Glacier near the midsummer transient equilibrium line in the vicinity of Slanting Peak on July 27. Profile VIII was carried out on July 29 and August 13 on the Matthes Glacier between Blizzard Peak and Mt. Moore. Profile X was done on July 30 on the divide between the Matthes from the Llewellyn Glaciers. Profile IX was completed on the Vaughan Lewis Glacier between Blizzard Peak and Camp 18 on August 5 and 6. Profile XII was carried out on August 9 and

Map Adapted from USGS Map "Juneau, Alaska-Canada" (Alaska Topographic Series)

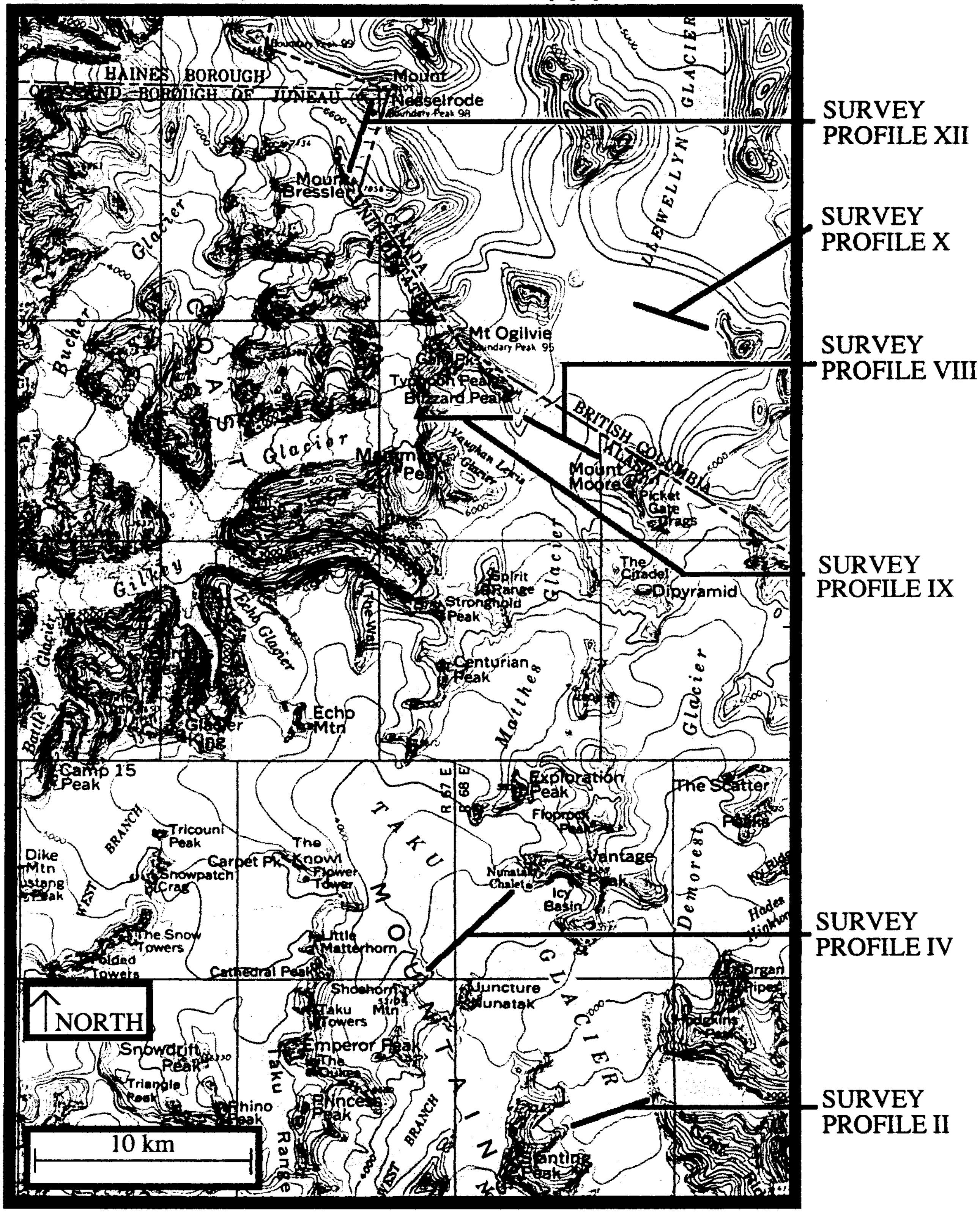

FIGURE TWO: SURVEY PROFILE POSITIONS

10 between Mt. Nesselrode and Mt. Bressler on the Bücher Glacier.

On each profile, seismic soundings were taken at survey positions (flags) which were surveyed using Global Positioning System (GPS) techniques (Table 1). Therefore the absolute surface position of each seismic sounding can be accurately determined. The only exception was the Bücher Glacier profile which could not be GPS surveyed because of weather conditions. However, conventional survey techniques were employed, and reasonable estimates of the shot positions for this profile have been made.

Equipment

The Juneau Icefield Research Program provided a Bison 9024 (DIFP) portable stacking seismograph and two lines of twelve geophones. Kinepak brand explosives were used in conjunction with DuPont seismic detonator caps. In addition a Bison battery-powered blasting box was employed. Morton Thiokol snow-transport vehicles were used for moving equipment and personnel.

Field Methods

In all of the 1993 seismic work the two geophone lines were connected together resulting in a configuration of twenty-four geophones on a single line.

TABLE ONE: POSITIONS OF SEISMIC SURVEY FLAGS

PROFILE VIII

FLAG NUMBER	EASTING (m)	NORTHING (m)	Elevation (m)
1	487763	6524125	1898
2	488063	6523894	1839
3	488351	6523675	1824
4	488610	6523476	1816
5	488826	6523311	1812
6	489050	6523141	1807
7	489261	6522980	1804
8	489470	6522821	1800
9	489690	6522653	1794
10	489896	6522497	1790
11	490097	6522344	1787
12	490354	6522147	1793
13	490580	6521975	1815

PROFILE IX

FLAG NUMBER	EASTING (m)	NORTHING (m)	Elevation (m)
1	485269	6524979	1760
2	485393	6524944	1757
3	485522	6524914	1754
4	485651	6524862	1751
5	485771	6524796	1749
6	485872	6524709	1748
7	486047	6524560	1745

PROFILE X

FLAG NUMBER	EASTING (m)	NORTHING (m)	Elevation (m)
1	490008	6526293	1878
2	490295	6526220	1874

PROFILE XII

FLAG NUMBER	Elevation (m)
1	2010
2	2020
3	2030
4	2040
5	2050
6	2060
7	2070

Because of weather conditions, Profile XII was not GPS surveyed. However, estimates were made with the understanding that the survey line generally follows the transect line between Mt. Nesselrode and Mt. Bressler. Flags were positioned approximately 250m apart with Flag 1 about 300m from Mt Nesselrode.

The spacing between geophones was 10m; therefore the total geophone spread was 230m from end to end.

The first two profiles studied (IV, II) were primarily exercises in trial and error. At least seven methods were tried out:

1. A sledgehammer and iron plate were used to generate seismic waves. Sledgehammer position was offset about 1-2m from the geophone line in a split-spread fashion.

2. Various amounts of Kinepak (1-10 charges) were placed directly on the snow surface and fired in a split-spread fashion with offsets of up to 100m from the geophone line. This technique was tried by Poulter in Antarctica during the Second Byrd Expedition (1950a), by Röthlisberger on Baffin Island (1955), and by Doell on the Salmon Glacier in British Columbia (1963).

3. In-line shots were attempted with various amounts of explosives (1-10 sticks of Kinepak) at the snow surface.

4. In-line shots with offsets of 100-1000m were carried out with 1-5 sticks buried about .5 m below the snow surface. A similar technique was used in the Antarctic by Robin (1952).

5. Split-spread shots with various offsets were done with 1-5 sticks buried at about .5m.

6. Split-spread shots were done with 1-5 sticks left in a open hole about

.5 m deep.

7. Split-spread shots with small offsets (less that 5m) were attempted with 1-5 sticks buried at 2-3m. This was Poulter's method of choice in Antarctica (1950a).

Experimentation with these six techniques on profiles II and IV produced almost fifty seismic records; however, none of them had clear reflecting waves. Because of this, trials were carried out with above-surface shots. This was done by attaching 1-5 Kinepak charges on a bamboo wand about 1-2m above the glacier surface in a split-spread fashion. This yielded better, though still vague, seismic records on Profiles II and IV. However, by the time the expedition had reached Profile VIII, this above-surface technique was refined enough so that clear reflections were being recorded.

The method of using a charge pattern suspended above the glacier surface was first studied by T.C. Poulter and consequently is called the "Poulter Seismic Method." Its main advantage over a buried shot is that it concentrates energy in the vertical direction, which enhances the signal-to-noise ratio and strengthens the reflection (Poulter 1950b). The most useful variation of the Poulter Method for the 1993 seismic work was found to be an above-surface shot with single charges mounted on three 1-2m bamboo wands arranged in a triangular fashion with each wand about 1m apart. This was done in a split-spread manner with the offset of the shot pattern from the geophone line between 80m and 200m (Figure 3). The best offset distance had to be found by trial and error at each sounding point, and it was also sometimes necessary to increase the amount of explosive to two sticks per wand. On the other hand, it was possible on some occasions to use only a single wand with one or two Kinepak charges. Again, this had to be ascertained at each sounding point by trial and error.

Velocity of the Compressional Wave in Ice

The velocity of the compressional wave in ice is of importance because it is the central constant in a seismic glacier depth analysis. In the literature there is a variety of measured velocities:

Brockamp and Mothes, Austrian Alps (1927)	3600 m/s
Goldthwait, Crillon and Klooch Glaciers, AK (1936)	3000 m/s - 4600 m/s
Peterson, Port Barrow AK (1949)	3750 m/s
Poulter, Taku Glacier AK (1950c)	3950 m/s
Robin, Antarctica (1952)	3800 m/s
Allen and Smith, Malaspina Glacier, AK (1953)	3755 m/s
Röthlisberger, Baffin Island (1955)	3760 m/s

Doell, Salmon Glacier, British Columbia (1963)	3660 m/s
Hobson and Jobin, British Columbia (1975)	3810 m/s

These velocities represent a mixture of data from polar, sub-polar, and temperate glaciers. The compressional (P-wave) velocity in polar glaciers is very well quantified and has been shown to be dependent on ice temperature (Kohnen 1974). However, the compressional wave velocity in temperate glaciers is also dependent on water content (Paterson 1981). This means P-wave velocity can vary between temperate glacier systems, implying that there is not a general value which can be applied in every situation. Therefore it was necessary for the 1993 geophysical team to establish its own P-wave velocity for survey use, and this was done by employing seismic techniques and radio-echo sounding methods together. On Profile X the radar produced convincing reflections, and since the propagation velocity of electromagnetic waves in ice is well-known, it was possible to calculate a reliable ice-depth. Since there were strong seismic reflections at the same position, a seismic compressional wave velocity of about 3660 m/s was deduced. Since this velocity is consistent with the findings of earlier workers, and since it is supported by this excellent radar evidence, 3660 m/s is used for all calculations in the analysis of the seismic records.

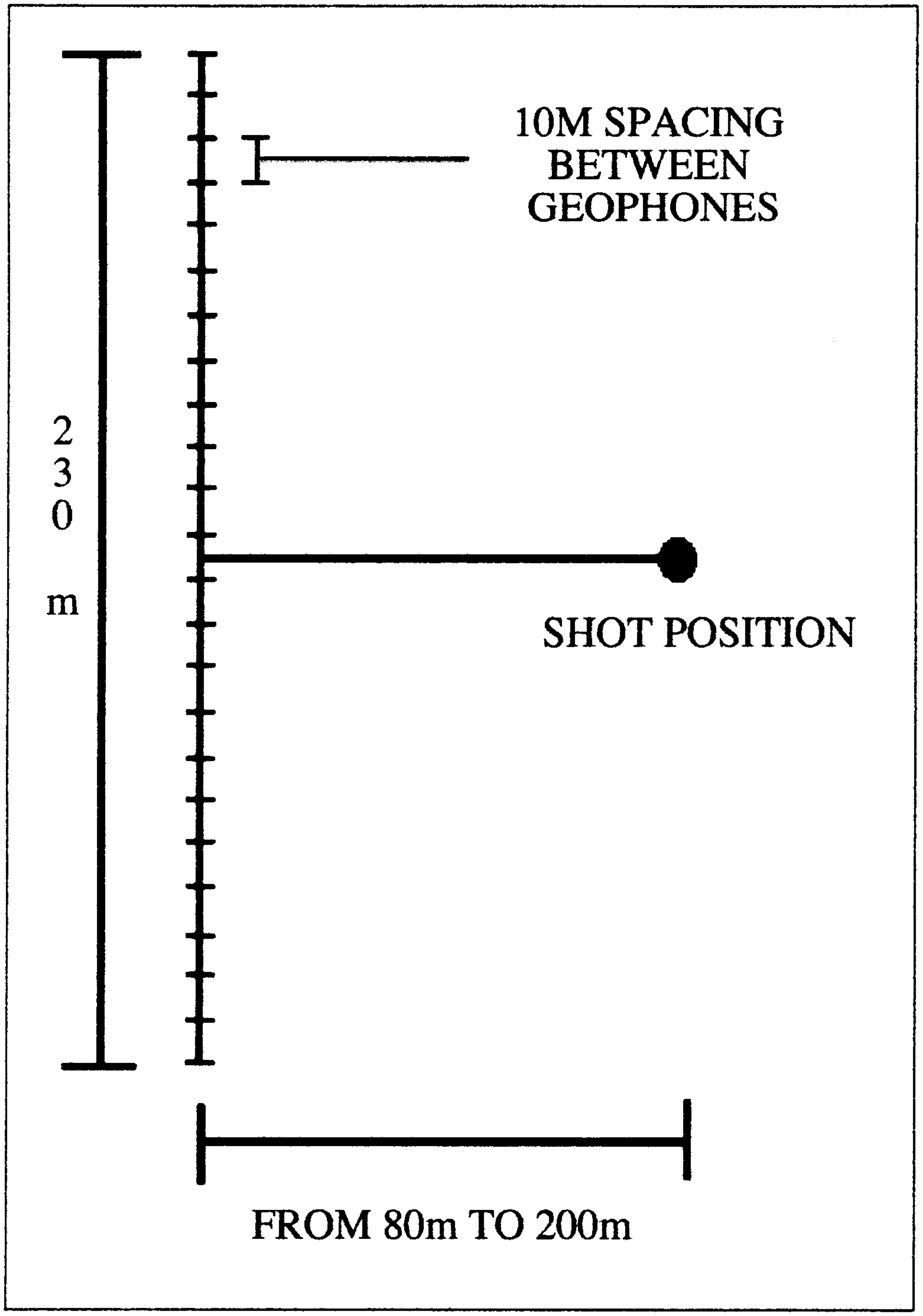

FIGURE THREE:
GEOPHONE/SHOT
PLACEMENT

Description of Seismic Records

Four primary types of waves are present in a typical 1993 seismic record: the P-wave, S-wave, reflected wave, and the air wave (Figure 4). Of these only the reflected wave arrived as a single pulse. The remaining waves each arrived in groups of three parallel pulses, a pattern which was repeated in all 1993 seismic records regardless of the geophone-shot configuration. This triple pattern is interpreted to result from the use of Kinepak explosive, which tends to burn less "cleanly" than other explosives, thus producing a multi-pulse waveform. Therefore each record is interpreted to have only <u>one</u> arrival each of a P-wave, S-wave, and air wave. In other words, the triple pulse pattern does not suggest three separate arrivals of each type of wave; instead, it is indicative of a single, odd-shaped wavefront which is the result of the Kinepak explosive.

The P-wave (first arrival) is interpreted as a compressional direct wave which in some cases became a refracted headwave because of the velocity contrast at the firn-ice interface. In areas where the firn layer was thin or non-existent, such as Profile II, no refraction was displayed because the entire first arrival was a direct wave propagating through ice. In records from higher elevations, where a considerable firn layer was present, the first arrival underwent a subtle, though definite, refraction. From calculations using

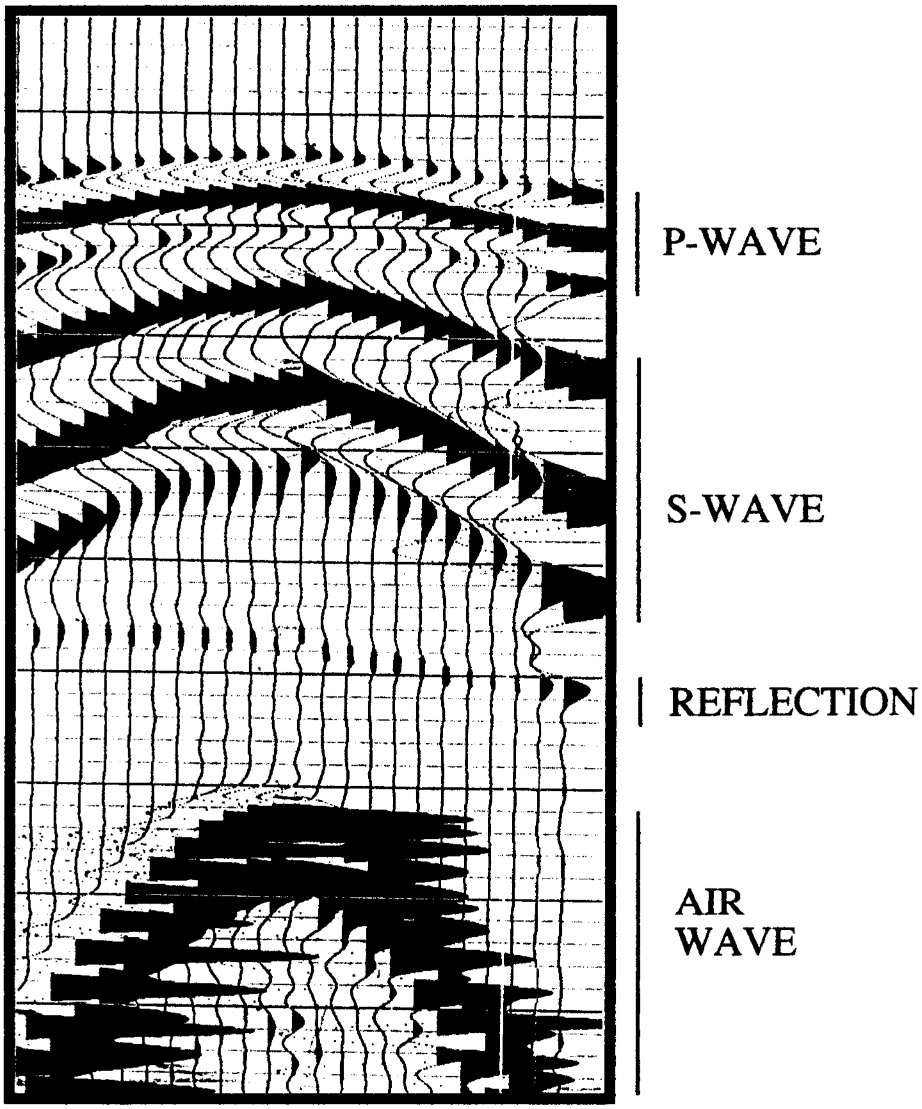

FIGURE FOUR: A TYPICAL SEISMIC RECORD (0046) conventional refraction analysis, the firn layer present at Profiles VIII, IX, X, and XII was measured to vary from 30m to 50m (Figure 5). The velocity of the compressional wave in the firn was calculated to be about 1500-2000 m/s, which is consistent with the findings of the Poulter survey (1950a). Using the same methods the compressional wave velocity in ice was measured to be 3000-4000 m/s. Although much less elegant, this is roughly consistent with the velocity determination carried out by radio-echo sounding.

At first glance the identity of the second arrival appears questionable as it could be interpreted as a shear wave or a surface wave. However, upon inspection it is clear that the second arrival undergoes refraction, which leads one to the conclusion that it must represent a shear wave. This conclusion is supported by Poulter (1950c) who stated that an air-shot creates vertical shear movement in the upper firn layer. This gives credence to the idea that shear motion could be detected by standard vertical-component geophones such as the type used by the 1993 seismic survey. Poulter also asserted that an air shot severely attenuates surface waves. This is consistent with the fact that if the second arrival is interpreted as a shear wave, then surface waves are completely absent from the 1993 seismic records

The reflected wave (typically the third arrival) is clear in most records but is almost always quite weak. Therefore filtering, mostly low-pass, was used as was automatic gain control (AGC) for strengthening the reflection.

FIGURE FIVE: REFRACTION ANALYSIS

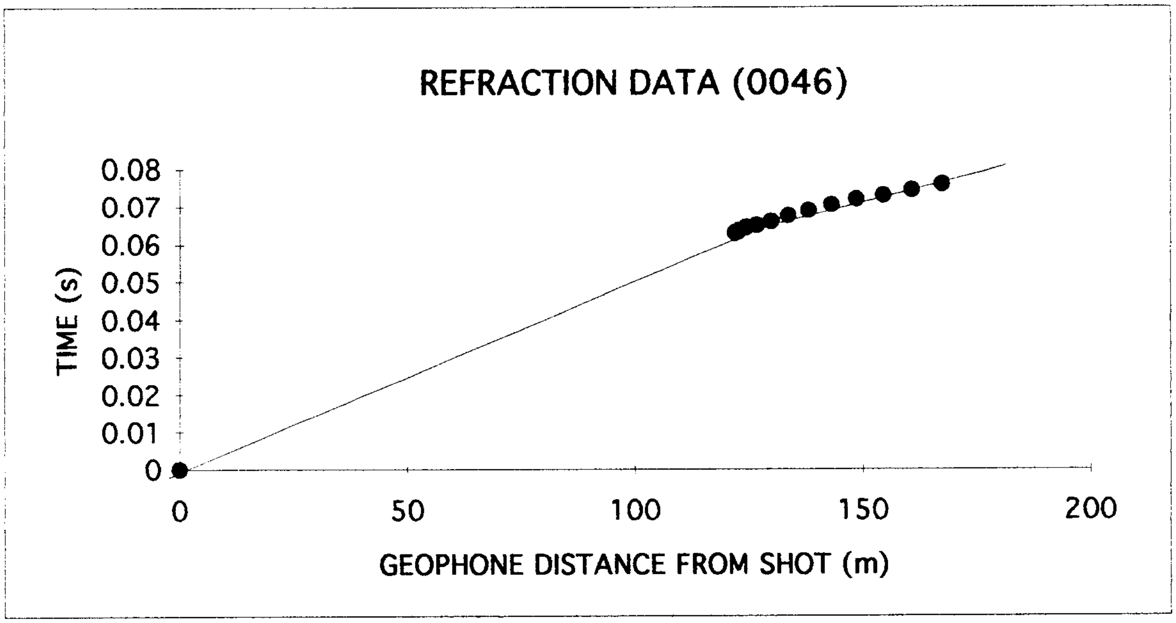

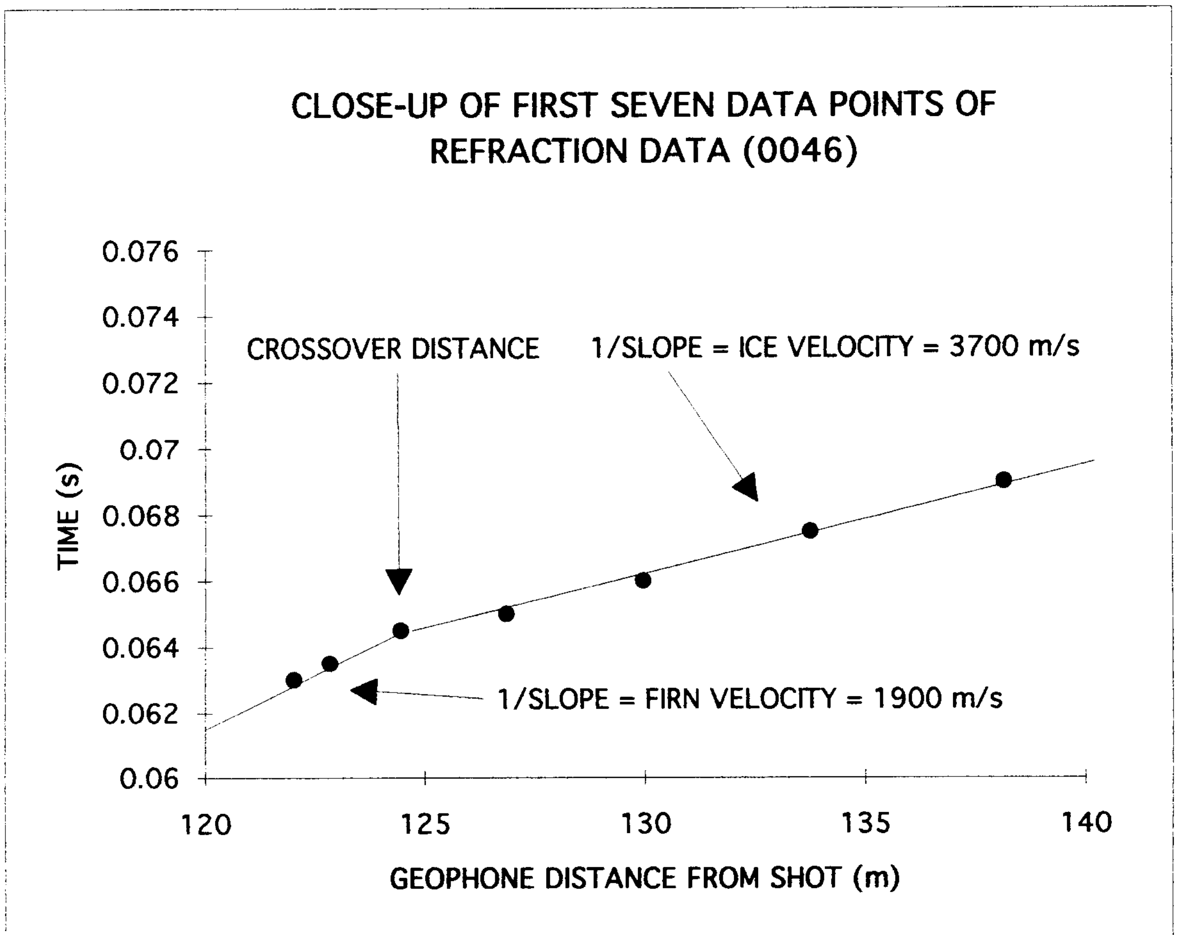

These efforts made reflections much easier to delineate, although the AGC greatly increased background noise.

Analysis of Reflection Data

In order for the position and orientation of a seismic reflecting surface (a glacier bed in this case) to be completely constrained in 3-D space relative to a shot point, a geophone array must be configured so that all of the geophones do not lie on a single line (Röthlisberger 1955). In order to achieve this, a "cross," "T," or triangle geophone pattern must be employed. However, because of time constraints and logistics, these configurations could not be used during the 1993 field season. Fortunately, even with a layout of in-line geophones, it is possible to estimate the orientation of a glacier bed and glacier depth if reasonable assumptions are made.

Consider two hypothetical bed orientations. The first possibility, a transverse dip, occurs when the glacier bed dips laterally under the geophone line. In other words, since the geophone line was almost always oriented perpendicular to glacier flow, this implies that the glacier bed in this case is dipping perpendicular to flow, across the glacier. The second possibility, a longitudinal dip, happens when the glacier bed dips perpendicular to the geophone line. In this configuration, if the geophone line is again oriented perpendicular to glacier flow, the glacier bed is seen to be slanting up-glacier or down-glacier with respect to the glacier surface. Obviously, in nature neither of these two situations exist by themselves. Instead they are end-members, and natural bed orientations are combinations of transverse and longitudinal dip components (Figure 6).

Since the 1993 seismic survey was completed with in-line geophones, it was not rigorously possible to deduce from a particular seismic record the complete description of bed orientation in terms of transverse and longitudinal dip. However, if one of these components can be taken to be negligible in comparison to the other, then a dip calculation could be made using only the "significant" component. In this analysis it was assumed that the transverse dip was much more important than longitudinal dip, and therefore the longitudinal dip was neglected. As can be seen in FIgure 6, this assumption is reasonable because the transverse dip represents the component of the bed orientation resulting from the curvature (U-shape) of the glacial valley. The longitudinal dip would seem to be small in comparison to this and therefore would have much less effect on the seismic records.

With this assumption a general travel-time equation was derived for the geophone-shot configuration used in 1993 in the case of a transverse-dipping glacier bed. (This derivation is tedious and is outlined in Appendix One) This equation can be varied to account for different shot offsets and bed dip

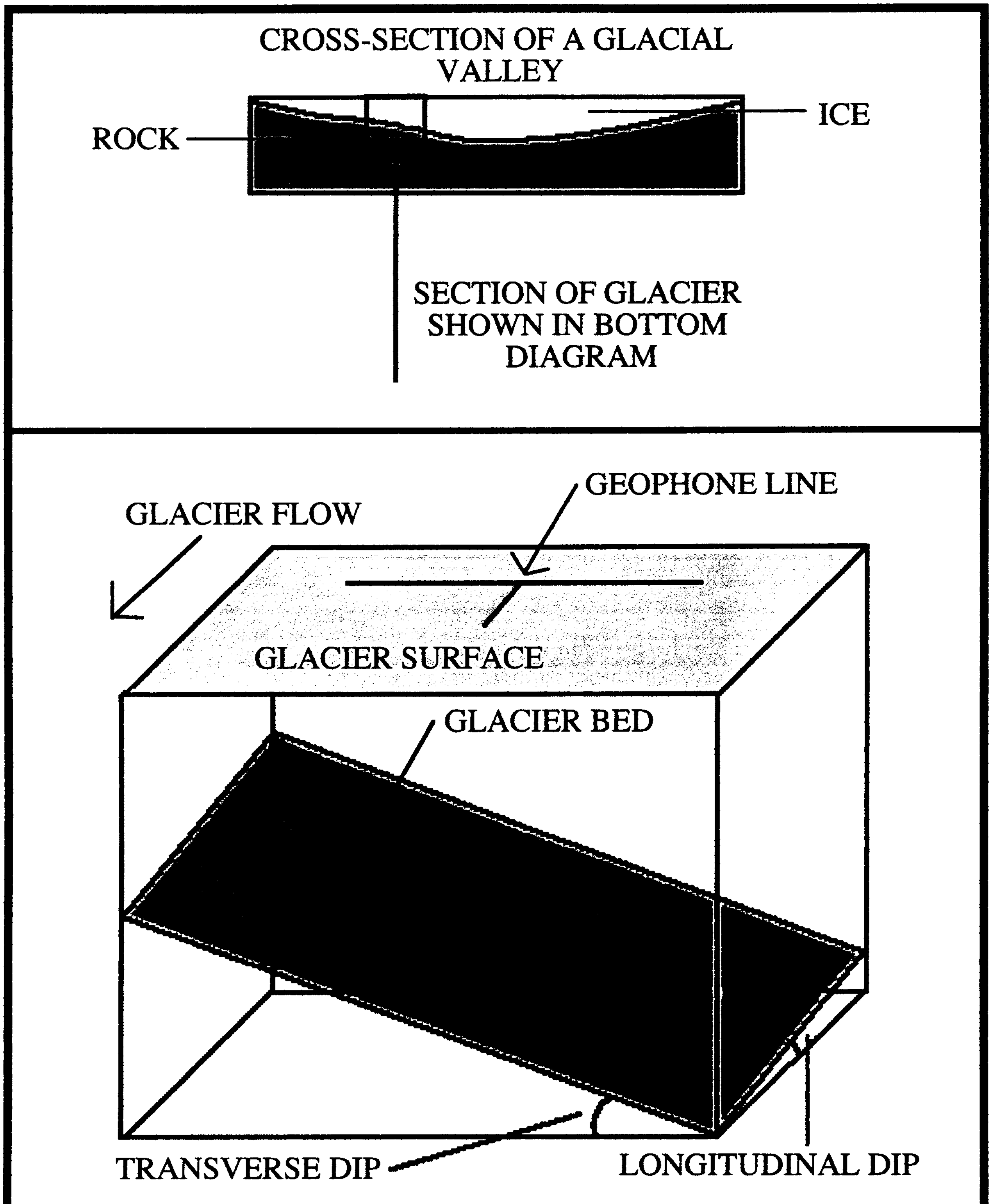

FIGURE SIX: DIAGRAM OF TRANSVERSE AND LONGITUDINAL DIP angles. Therefore theoretical reflection arrival times can be derived for a particular bed orientation and shot configuration, and then the reflection data from an actual field record can be compared with the theoretical curve.

The data analysis for each individual record was done by first picking the arrival of the reflected wave at the center geophone. This value, in addition to the offset distance, was entered for each record into a Microsoft Excel™ spreadsheet program designed to numerically solve the transverse travel-time equation. Using this program several travel time equations portraying different transverse dip angles were drawn for each record, and the curve of best fit was then manually chosen. With this completed, the glacier bed orientation is then known, and the glacier depth can be calculated using simple geometric relationships.

An example of this treatment of the problem can be examined in Figure 7. In this case, the arrival time at each geophone of the reflected wave in Record 0048 is graphed against geophone position relative to the center of the array. (For example, the reflected wave arrival time at geophone # 1 is graphed at x = 115, the arrival time at geophone # 2 is plotted at at X = 105, and the arrival time at geophone # 24 is graphed at X = -115.) In addition, the curve representing theoretical arrival times for a bed oriented at 13° is plotted in the same manner. Since this curve correlates reasonably well with the field data, the glacier bed in Record 0048 is consequently estimated to be

FIGURE SEVEN: AN EXAMPLE OF A BEST FIT TRAVEL-TIME CURVE

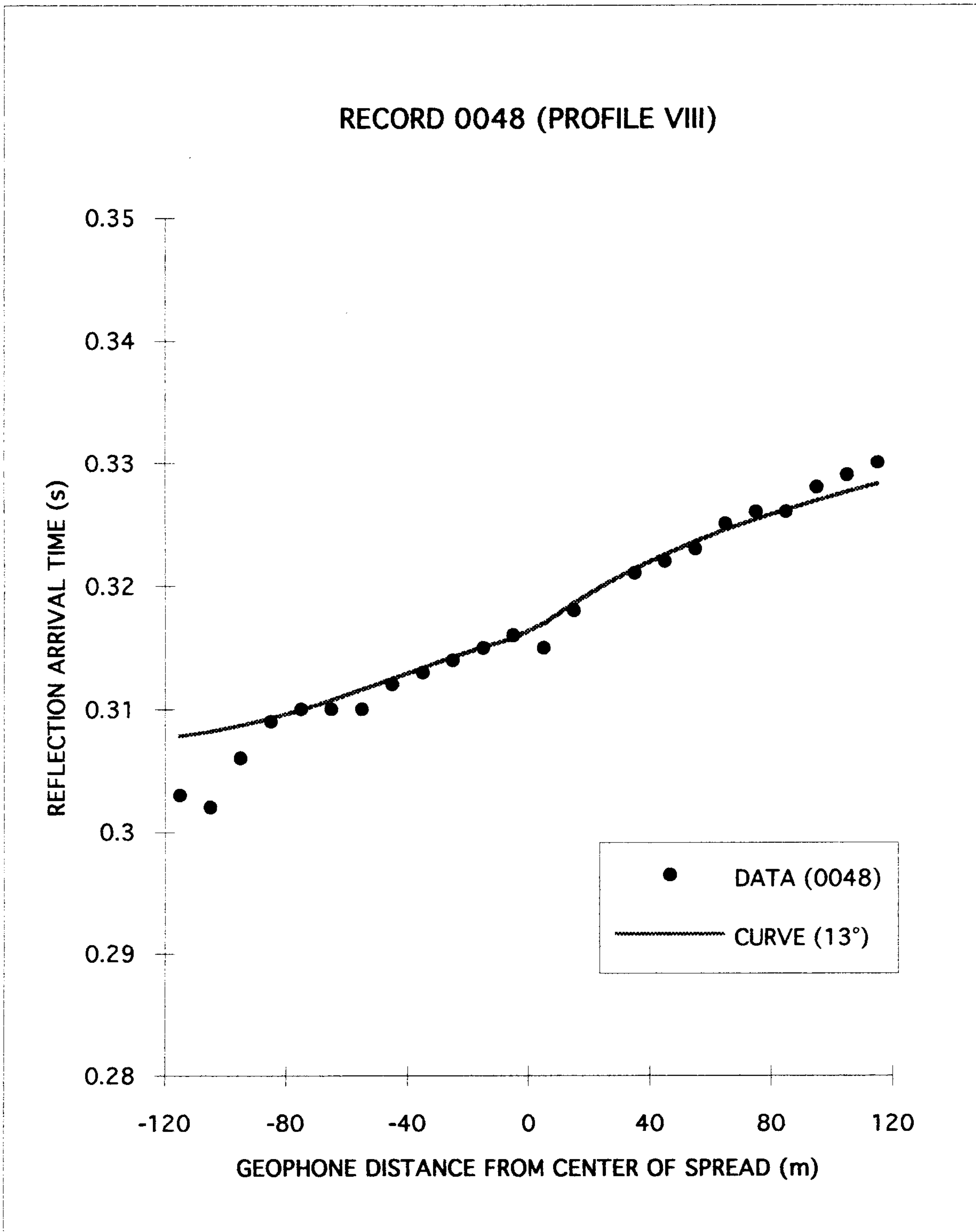

oriented at 13°.

This analysis was done for each available record which had a reflection covering at least 10 channels (see Figures in Appendix Two). (Records with a reflection of spread over less than 10 channels could be fit to a curve; however, having so few data points in most cases caused the curve/data correlation to become quite ambiguous.) If a record did not qualify for dip analysis, two approaches were used. First, if there were multiple records taken at a single position, and if only one of these records had enough data points for a dip analysis, then the calculated dip for that record was used in the analysis of all of the "poorer" records at that position. Second, if none of the records at a single position have enough data points, then the glacier bed was assumed to be flat and the depth was estimated using depth $= \sqrt{(V_oT_o)^2 - X^2)}/2$ where V_o = velocity of ice, T_o = time of reflection arrival at center geophone, and X = offset distance. The results of the analysis of the records from Profile VIII, IX, X, XII are presented in Table 2. Since no creditable reflections were produced at Profiles II and IV, depth data from those profiles is not included.

Reliability of Results

The reliability of the depth calculation is mostly linked to the trustworthiness of the raw reflection data, which in turn is dependent on two

TABLE TWO: BED ORIENTATION AND DIP CALCULATIONS

PROFILE VIII	Record	Depth (m)	Dip Angle
Flag 4	0042	510	
	0046	530	14
Flag 4a	0047	550	15
Flag 4b	0048	590	13
Flag 9	0190	805	
	0194	825	
	0200	805	16
Flag 11	0203	645	20
	0205	645	
	0208	610	
	0208	630	

In Profile VIII "4a" is centered 115m towards Flag 5 from Flag 4,. and "4b" is centered 230m from Flag 4.

PROFILE IX	Record	Depth (m)	Dip Angle
Flag 3	0097	520	
	0099	450	13
Flag 5	0076	480	
	0077	460	11
Flag 6	0091	485	
	0095	450	0
Flag 7	0078	470	
Flag 8	0108	510	
	0110	460	8

TABLE TWO: BED ORIENTATION AND DIP CALCULATIONS (CONTINUED)

PROFILE X

	Record	Depth (m)	Dip Angle
Flag 1	0050	620	13
	0051	600	12
	0052	600	
	0056	600	11
Flag 2	0059	700	13

PROFILE XII

	Record	Depth (m)	Dip Angle
Flag 2	0112	520	
	0120	470	
Flag 3	0148	380	
	0145	370	
	0150	380	
	0153	380	
	0154	360	
Flag 4	0138	400	8
	0140	440	
	0143	400	
Flag 5	0159	410	
	0161	410	13
Flag 6	0164	360	
	0167	360	

main error factors: human error in picking reflections and machine errors in recording the seismic records. The human error is difficult to quantify; however, if it is assumed that the correct reflection wavefront was chosen in each record, then the error in measuring the arrival time of this reflected wave should not exceed about .025s. This translates into roughly an error of about ±40m meters in the depth measurement.

Machine errors, assuming all equipment was working properly, were probably negligible compared to human errors. However, the seismic survey did encounter a malfunction in the blast box which disabled the mechanism that triggered the seismograph upon shot detonation. This meant the seismograph had to be manually triggered on Profiles IX and XII, which implies that "time zero" on those seismic records was inaccurate. To compensate for this, the shot offset distance was measured, and then by using 343 m/s for the speed of sound, "time zero" was defined by measuring backward from the air wave arrival at the center geophone. (In other words, if the offset was 200m, the time required for the air wave to arrive at the center geophone is 200m/(343m/s) = .58s. Therefore "time zero" on that seismic record is defined as being .58s in front of the air wave arrival at the center geophone.) This obviously introduced many additional errors into the analysis. Roughly estimating, this suggests that arrival times could be inaccurate by as much as .1s. This translates into a possibility for almost ±150m error in the depth calculations for Profiles IX and XII.

This analysis of the error in Profiles IX and XII is very pessimistic, and it might have rendered the data meaningless if multiple shots had not been recorded at several flags on each profile. On both Profiles IX and XII, records taken at the same flag position result in depth calculations which correlate much better than ±150m. In most cases, even though the offset distance was varied for many of the records, the depth calculations mostly agree to within about ±50m. Since each one of these record analyses is independent, this implies that the error in depth calculation in Profiles IX and XII is much less than ±150m and is probably closer to ±50m.

The reliability of the dip calculation must be examined differently because the dip calculation is much less dependent on the accuracy of arrival time measurement than the depth calculation. This is because the dip calculation is contingent on the relative difference between reflection arrival times at different geophones. Therefore machine or human errors, if they were made consistently, should not effect the dip calculation. However, in all profiles the trustworthiness of the dip calculation is strongly linked to the accuracy of the assumption that the longitudinal dip of the glacier bed was small enough to be negligible. If this premise is significantly incorrect, then the reliability of the dip calculation will be much reduced.

Conclusion

Seven main conclusions can be drawn from the 1993 Seismic Survey on the Juneau Icefield:

1. Radar and seismic work in conjunction indicates that the velocity of the compressional wave in ice for the Juneau Icefield glacier system is approximately 3660 m/s.

2. Refraction analysis indicates that firn layer depths on Profiles VIII and X are between 30-50m, and the speed of the compressional wave in firn is about 1500-2000m/s

3. No clear reflections were produced on Profiles II and IV by the Poulter Methods which later produced clear reflections on profiles VIII, IX, X, and XII. This implies that the reflections on Profile II and IV were obscured by the first and second wave arrival. Since these waves arrive quite early on the record, this means that the reflection must be from a shallow source, indicating that the depth of glacier bed is probably not greater than 400-500m. This conclusion supports Poulter's findings on Profile II an IV in the 1949 survey and contradicts Nolan's findings in the 1992 survey.

4. Profile VIII (Upper Matthes Glacier) is viewed as having depths of about 500m on the western section of the profile with a bed orientation of about 15°. The depth increases toward the center of the glacier and probably

reaches its maximum around Flag 7. By Flag 9 the dip angle has reversed, and the glacier depth is about 800m. As the profile extends farther east toward Flag 13 the depth decreases. (Figure 9)

5. Profile IX (Vaughan Lewis Glacier) is characterized by glacier depths of about 450m (Figure 8).

6. Profile X (the divide between Matthes and Llewellyn Glaciers) is characterized by depths of 600m at flag 1 and 700m and flag 2. Dip angles are 10-15°. (Figure 10)

7. Profile XII (Bücher Glacier) is characterized by depths of about 400m. (Figure 11)

Acknowledgments

We would like to thank Dr. M. M. Miller, director of JIRP, who initiated this study and provided much-needed field guidance and support. We also acknowledge Dr. Ken Sprenke and Bob Hammond for their direction during the survey. Dr. Val Chandler, Minnesota Geological Survey, also provided assistance in interpreting the seismic records. Carl Coryell-Martin deserves thanks for his work on the ice radar. Gretchen Staeheli merits accolades for putting up with the geophysics crew for an entire summer. We also thank Mrs. Joan Miller for her hard work in providing critical logistical support. Lastly, those of us who received grants and scholarships from NSF and other sources through the Foundation for Glacier and Environmental Research wish to say thanks for their very generous support.

FIGURE EIGHT: CROSS SECTION OF PROFILE VIII

(UPPER MATTHES GLACIER)

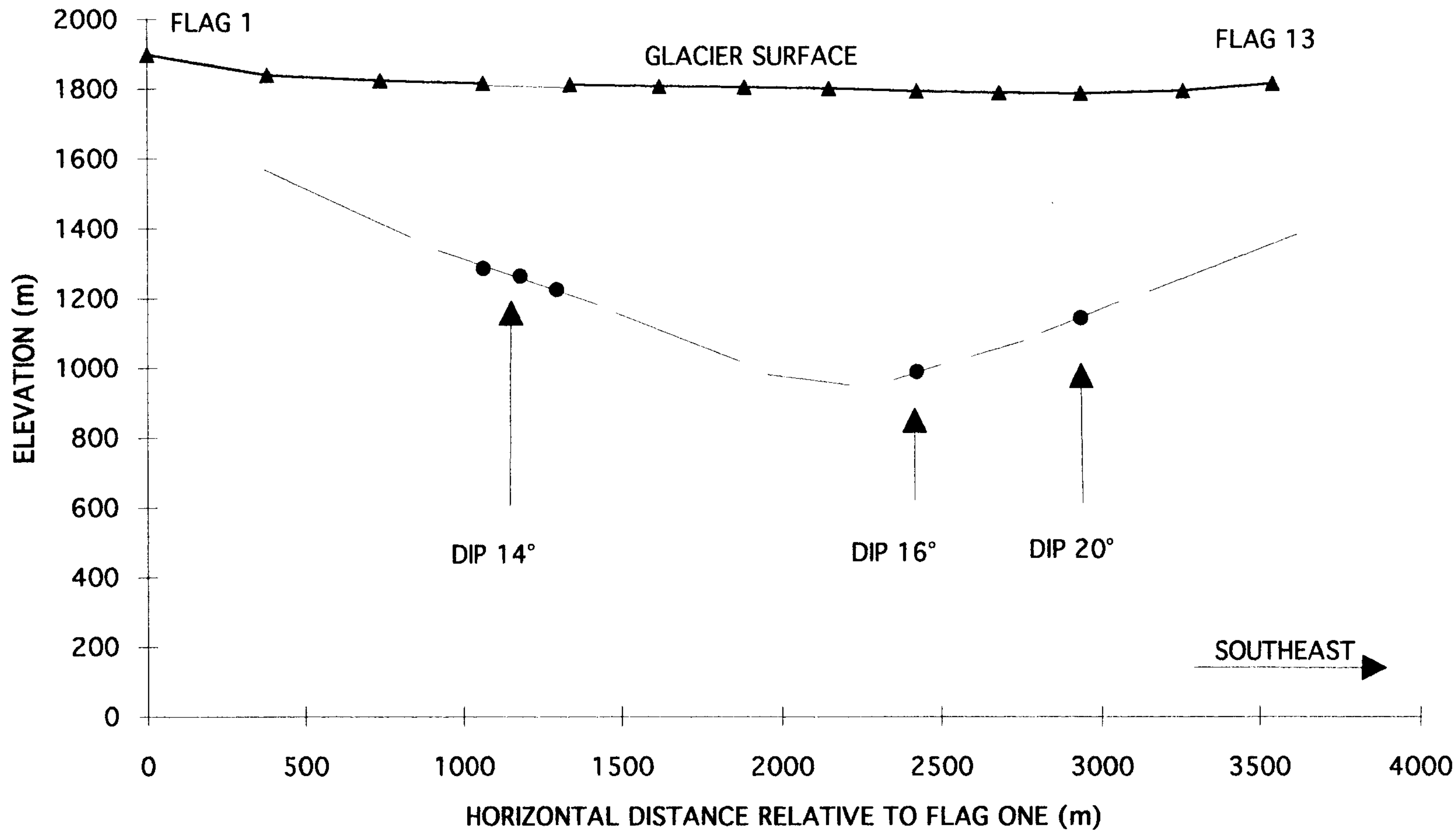

FIGURE NINE: CROSS SECTION OF PROFILE IX

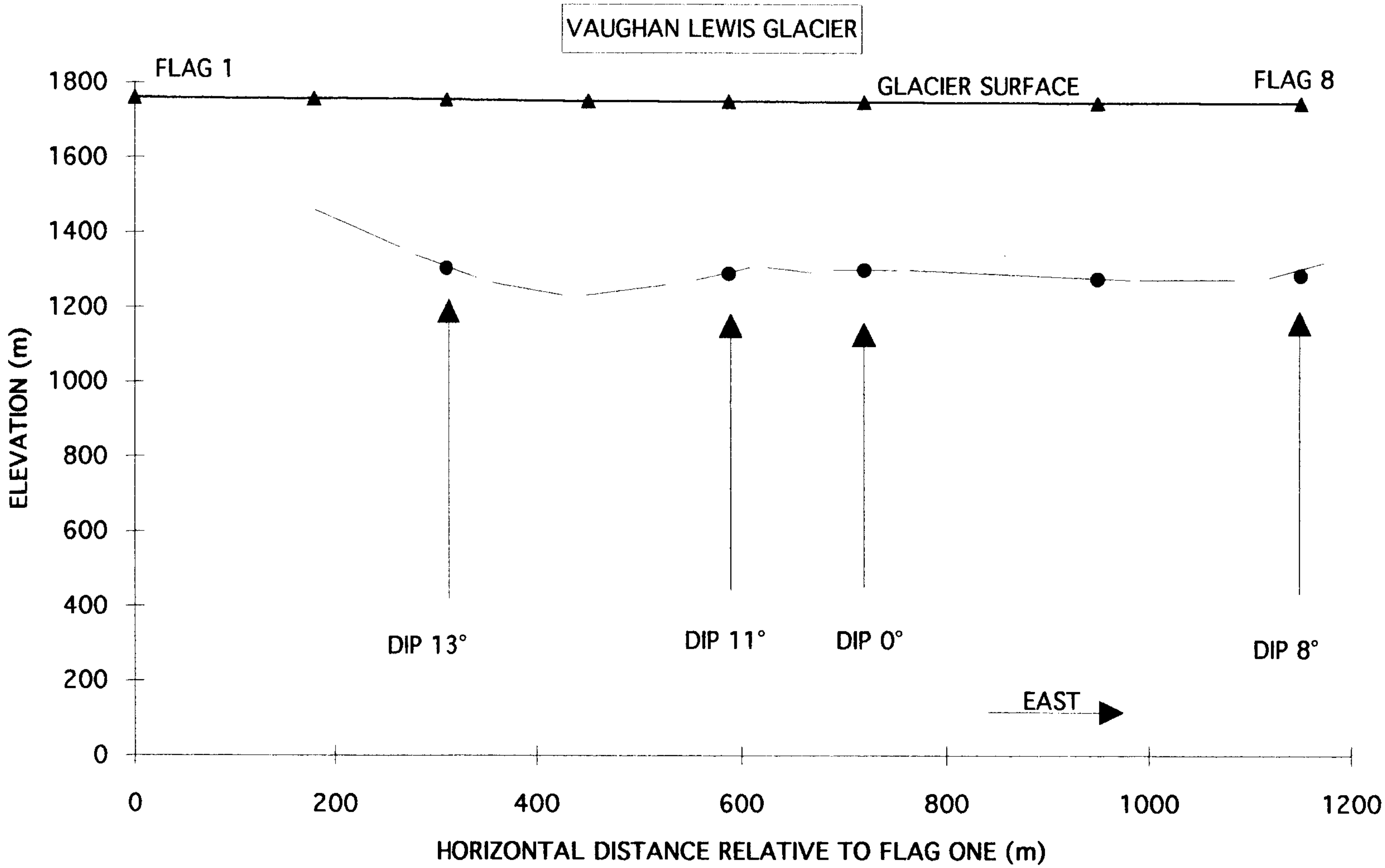

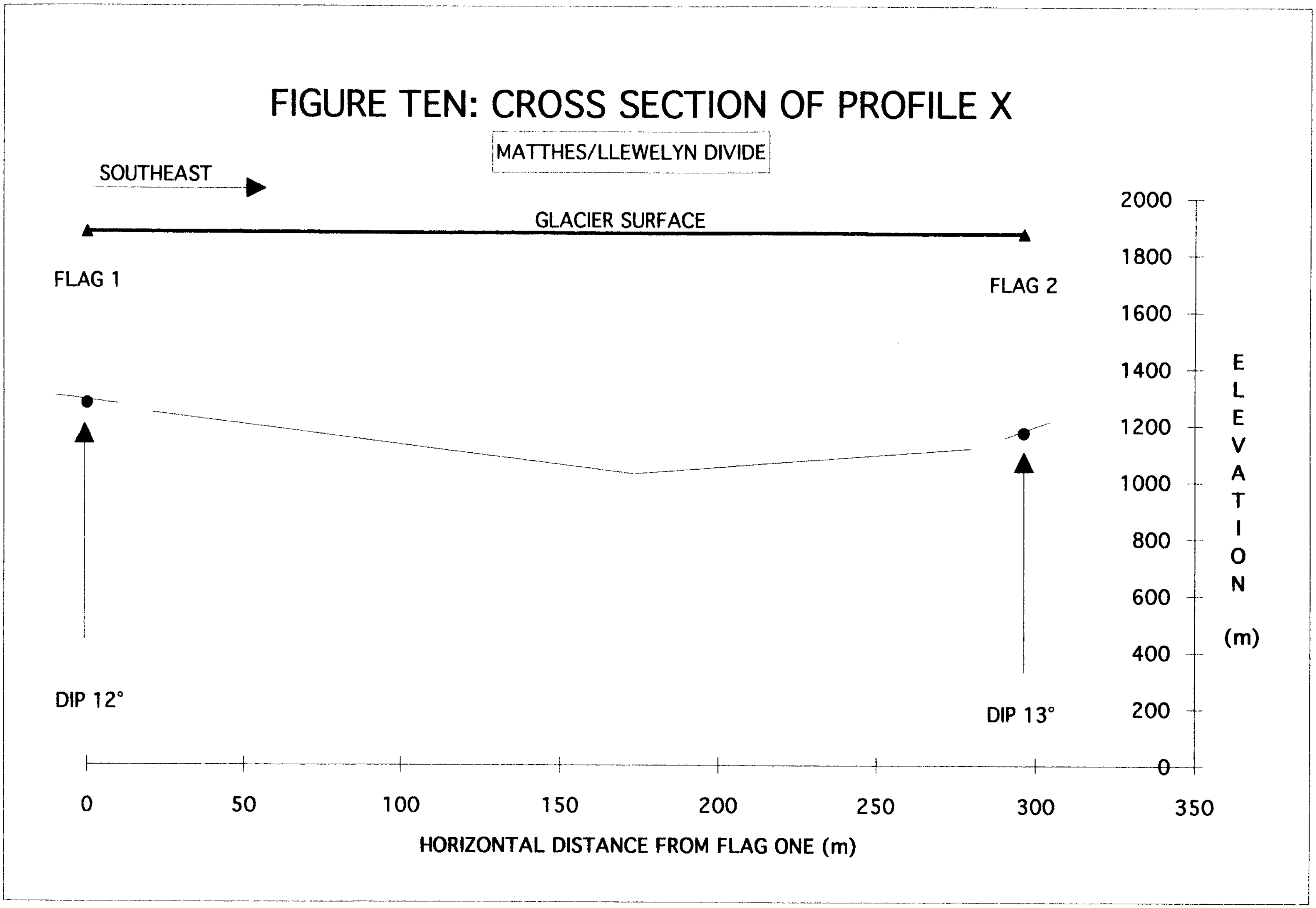
FIGURE TEN: CROSS SECTION OF PROFILE X
MATTHES/LLEWELYN DIVIDE
SOUTHEAST
GLACIER SURFACE
FLAG 1
FLAG 2
DIP 12°
DIP 13°
2000
1800
1600
1400
1200
1000
800
600
400
200
0
ELEVATION (m)
0
50
100
150
200
250
300
350
HORIZONTAL DISTANCE FROM FLAG ONE (m)

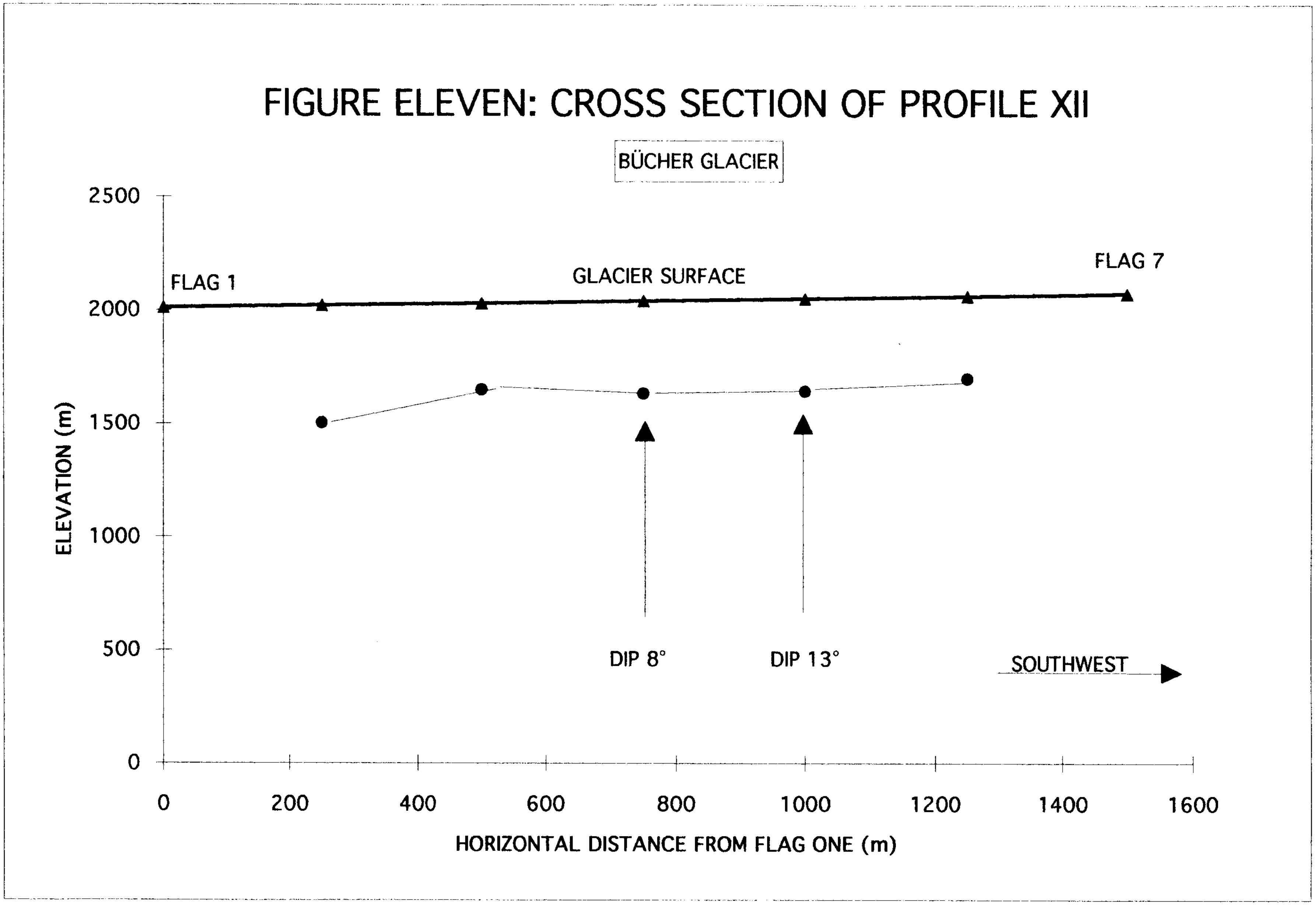

FIGURE ELEVEN: CROSS SECTION OF PROFILE XII
BÜCHER GLACIER
FLAG 1
GLACIER SURFACE
FLAG 7
DIP 8°
DIP 13°
SOUTHWEST
ELEVATION (m)
2500
2000
1500
1000
500
0
0
200
400
600
800
1000
1200
1400
1600
HORIZONTAL DISTANCE FROM FLAG ONE (m)

APPENDIX ONE

Outline of the Derivation of a Time-Travel Equation for a Transverse Dipping Glacier Bed for the 1993 Geophone-Shot Configuration

DERIVATION

Define:

t_o = time required for reflected wave to reach center geophone

V_o = velocity of compressional wave in ice

X = offset distance from shot to center geophone

d_i = distance from geophone (i) to center of geophone line

(for example: d_1 = 115m, d_2 = 105m ....d_{24} = -115m)

$D_i = \sqrt{(X^2+d_i^2)}$ = distance from shot to geophone (i)

∂ = true dip of glacier bed

Step One:

$h = \sqrt{((V_o t_o)^2 - X^2)}/2$ = distance from shot to bed in plane defined by shot position, center geophone, and a line perpendicular to bed

Step Two:

$H = h/\cos \partial$ = distance from shot to bed in plane defined by shot position, center geophone, and a line perpendicular to surface

Step Three:

μ = apparent dip = $\sin^{-1}(\cos \Delta \sin \partial)$

Δ = angle between shooting line and direction of true dip

$\Delta_i = \tan^{-1}(X/d_i)$

Therefore:

$$\mu_i = \sin^{-1}(\cos(\tan^{-1}(X/d_i))\sin\partial)$$

This step characterizes the apparent dip of the glacier bed underneath a line defined by a geophone and the shot position. Because of the geophone-array configuration, a raypath traveling from the shot to a geophone contends with a different apparent dip on the glacier bed for each individual geophone. Therefore, since there are 24 geophones, this apparent dip expression defines 24 equations, i.e. an apparent dip for each geophone.

Step Four:

$$S_i = H(\cos\mu_i)(\cos(\partial-\mu_i))$$

This step defines "S_i" as distance from shot to bed in plane defined by shot position, a geophone (i) and a line perpendicular to the bed. Note that for the center geophone, $\mu = \partial$, and therefore S = h

Step Five:

The classical time-travel equation for a dipping reflector, which can be found in a general geophysics textbook is defined as:

$$(Vt)^2 = 4A^2+W^2+2AW\sin\Sigma$$

where V = velocity, t = time, A = distance from shot to bed in plane defined by shot position, geophone, and a line perpendicular to the bed, W = distance from shot to geophone, and Σ = dip of reflector under line connecting shot position and geophone

Step Six:

By the substitution, and solving for "t," the classical equation becomes:

$$t_i = \sqrt{(4S_i^2+(D_i)^2+2S_i(D_i)\sin\mu_i)}/V_o$$

This expression represents 24 equations (one for each geophone). However, note that for a particular shot offset, compressional wave velocity, geophone, and true dip, this equation can be solved for a specific, numerical time. A Microsoft Excel™ spreadsheet program was then designed to calculate "t" given a particular shot offset, compressional wave velocity, geophone, and true dip. Using this program, an X vs t graph could made for the entire geophone array for a particular true dip. If this curve did not fit the field data, another true dip would be tried, and this process would be repeated until a good fit was found. Once the best fit true dip was found, the depth of the glacier midway between shot and the center geophone was calculated by:

$$\text{depth} = (\sqrt{((V_o t_o)^2 - X^2)}/2)/\cos\partial$$

APPENDIX TWO

Graphs of Data from Records and Corresponding "Best Fit" Travel-Time Curves

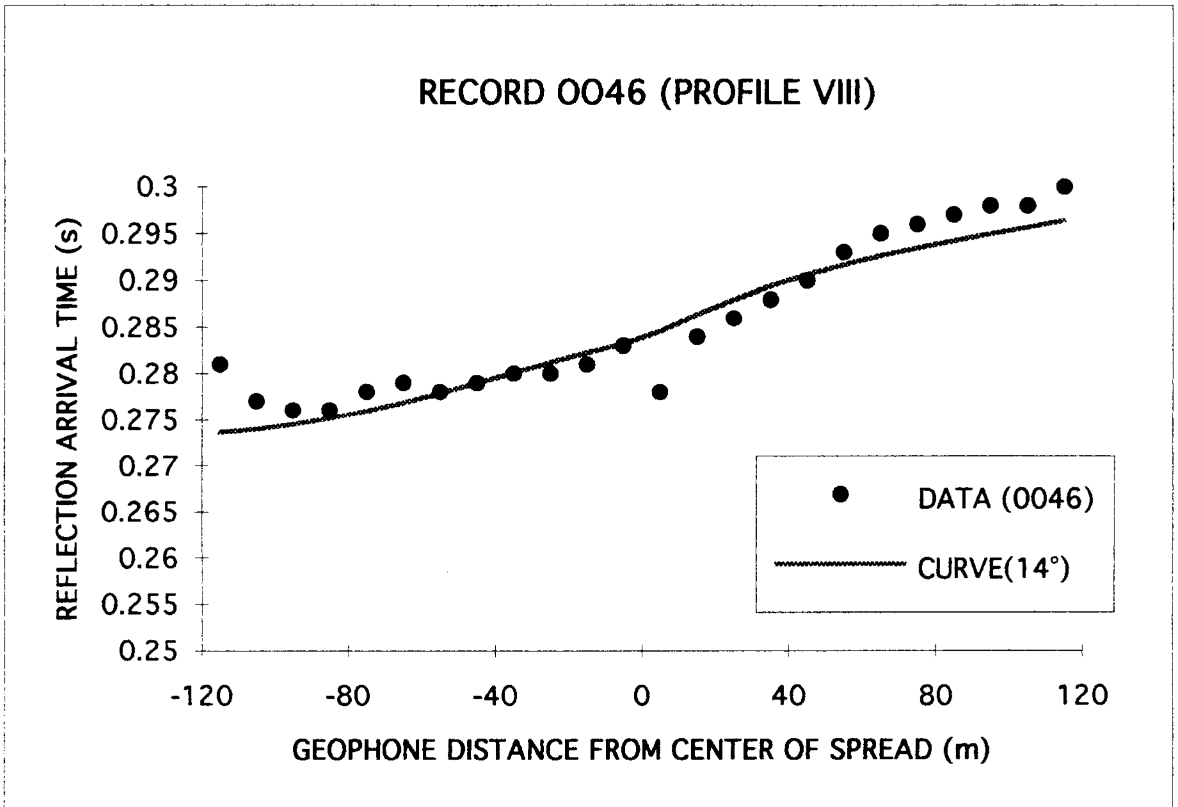
RECORD 0046 (PROFILE VIII)
REFLECTION ARRIVAL TIME (s)
0.3
0.295
0.29
0.285
0.28
0.275
0.27
0.265
0.26
0.255
0.25
-120
-80
-40
0
40
80
120
GEOPHONE DISTANCE FROM CENTER OF SPREAD (m)
DATA (0046)
CURVE(14°)

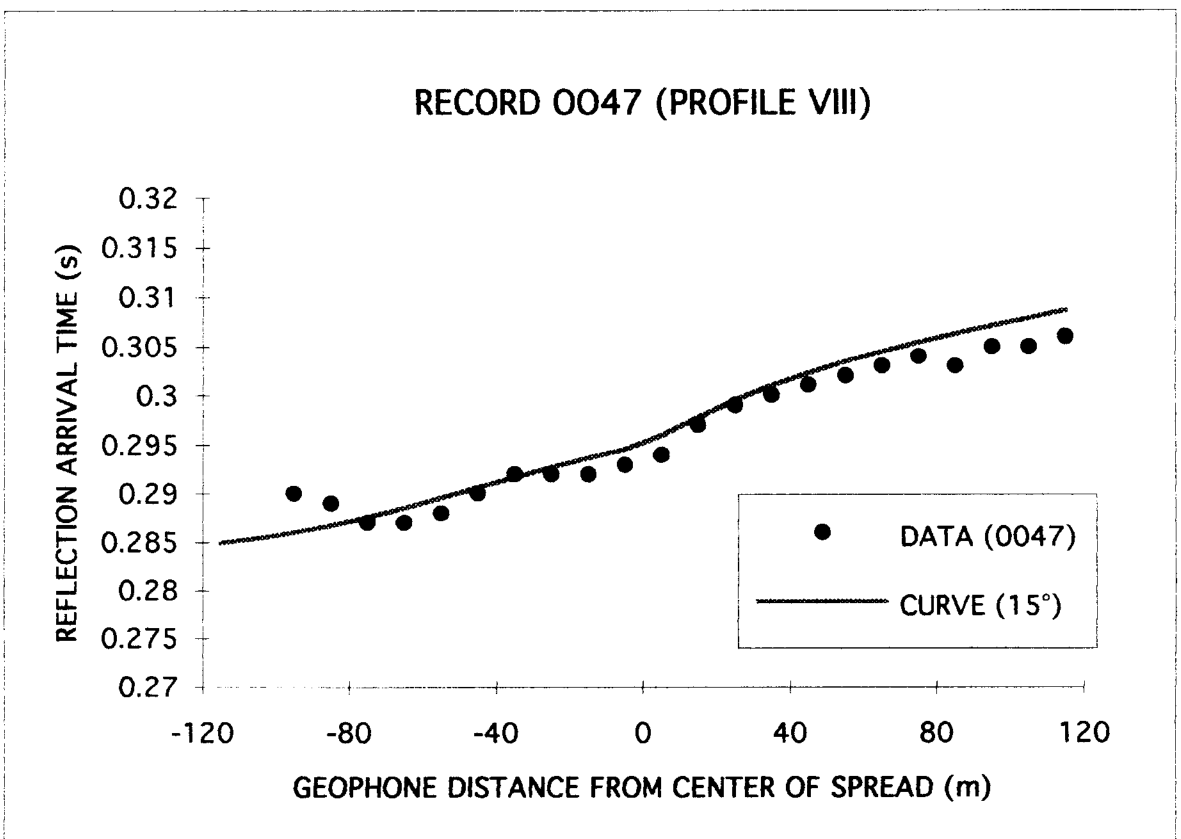
RECORD 0047 (PROFILE VIII)
REFLECTION ARRIVAL TIME (s)
0.32
0.315
0.31
0.305
0.3
0.295
0.29
0.285
0.28
0.275
0.27
-120
-80
-40
0
40
80
120
GEOPHONE DISTANCE FROM CENTER OF SPREAD (m)
DATA (0047)
CURVE (15°)

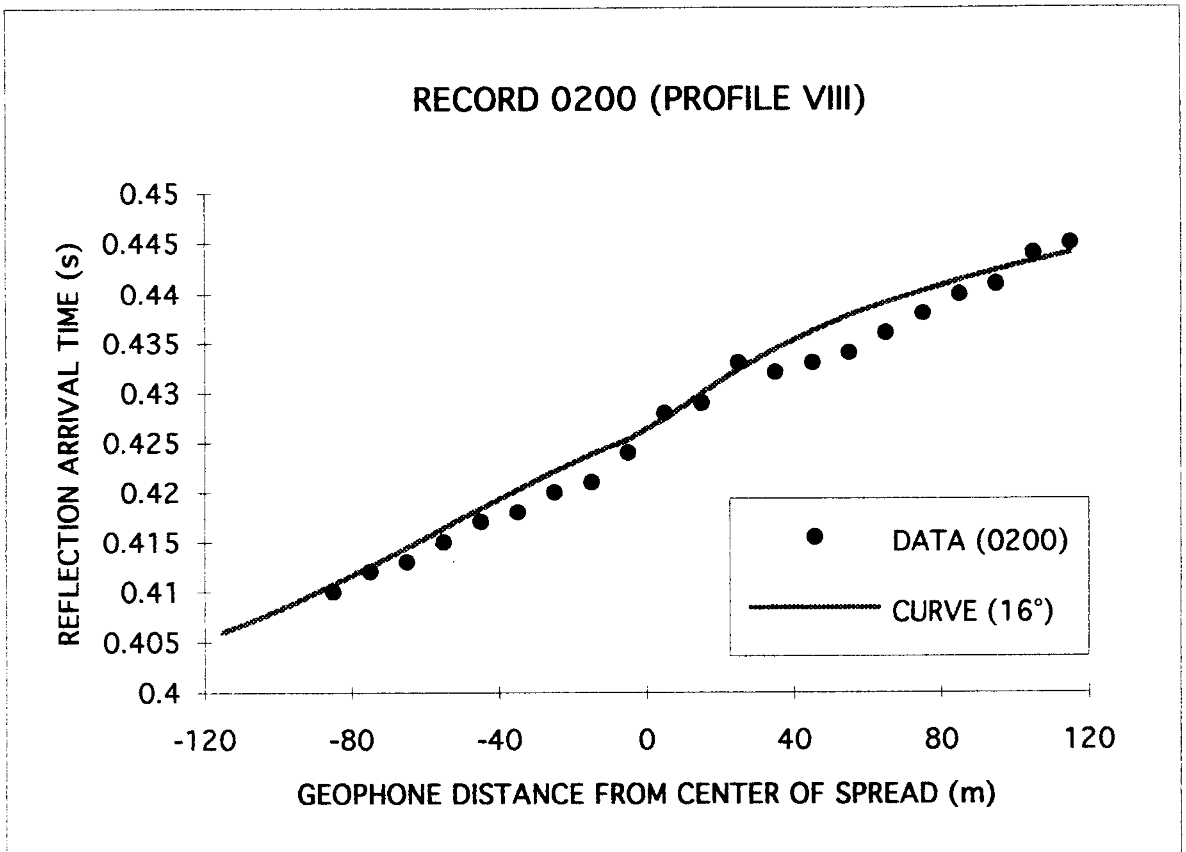

RECORD 0200 (PROFILE VIII)
REFLECTION ARRIVAL TIME (s)
0.45
0.445
0.44
0.435
0.43
0.425
0.42
0.415
0.41
0.405
0.4
-120
-80
-40
0
40
80
120
GEOPHONE DISTANCE FROM CENTER OF SPREAD (m)
DATA (0200)
CURVE (16°)

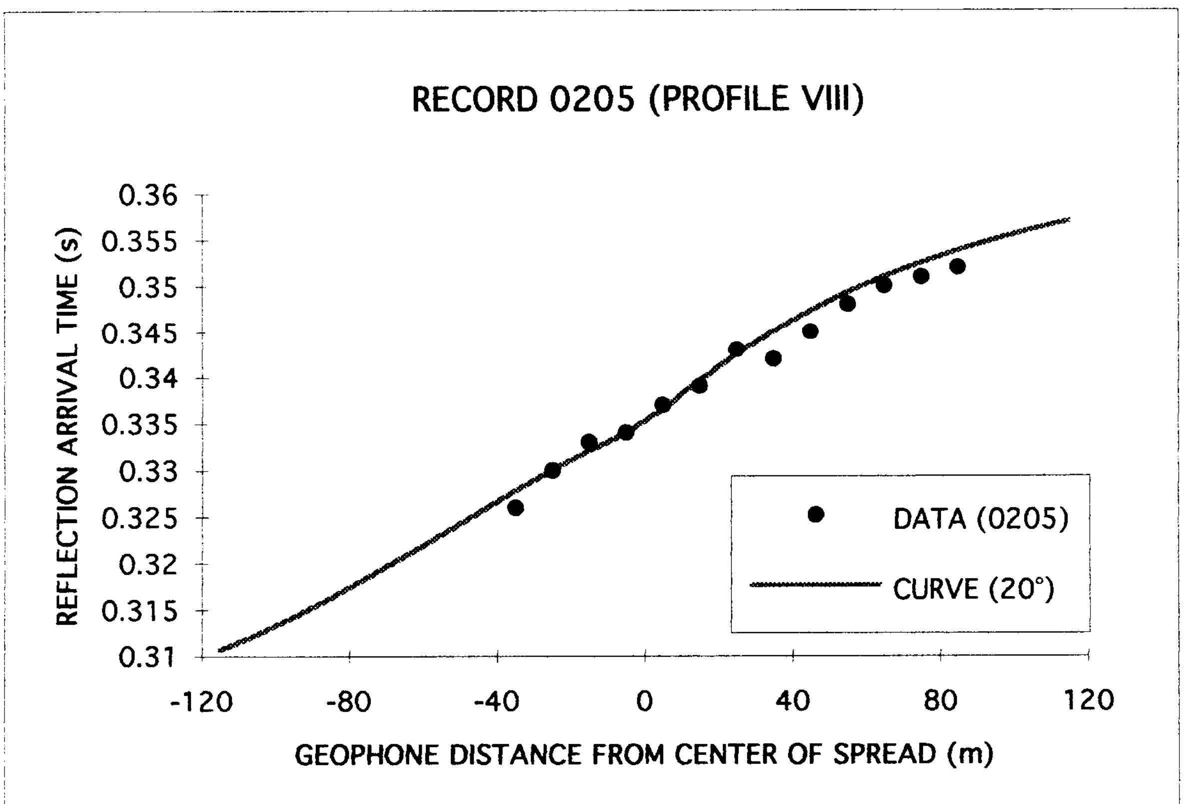

RECORD 0205 (PROFILE VIII)
REFLECTION ARRIVAL TIME (s)
0.36
0.355
0.35
0.345
0.34
0.335
0.33
0.325
0.32
0.315
0.31
-120
-80
-40
0
40
80
120
GEOPHONE DISTANCE FROM CENTER OF SPREAD (m)
DATA (0205)
CURVE (20°)

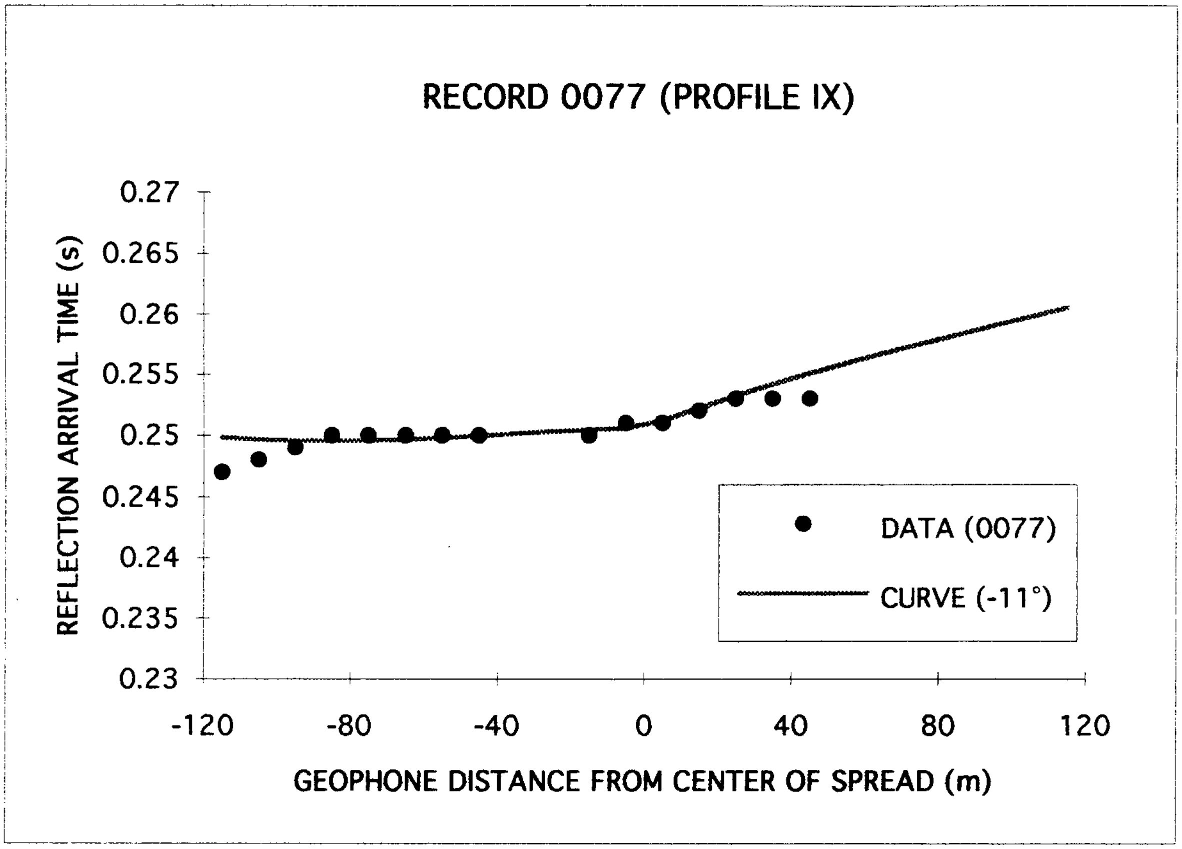
RECORD 0077 (PROFILE IX)
REFLECTION ARRIVAL TIME (s)
0.27
0.265
0.26
0.255
0.25
0.245
0.24
0.235
0.23
-120
-80
-40
0
40
80
120
GEOPHONE DISTANCE FROM CENTER OF SPREAD (m)
DATA (0077)
CURVE (-11°)

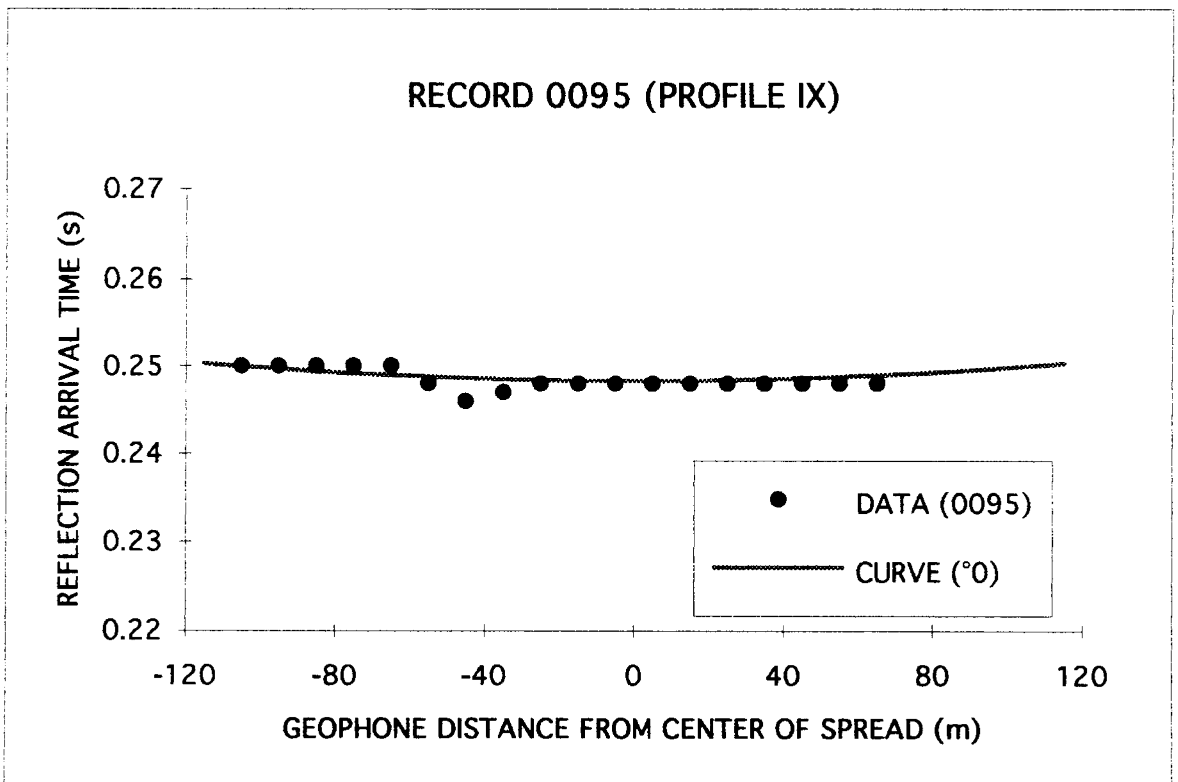
RECORD 0095 (PROFILE IX)
REFLECTION ARRIVAL TIME (s)
0.27
0.26
0.25
0.24
0.23
0.22
-120
-80
-40
0
40
80
120
GEOPHONE DISTANCE FROM CENTER OF SPREAD (m)
DATA (0095)
CURVE (°0)

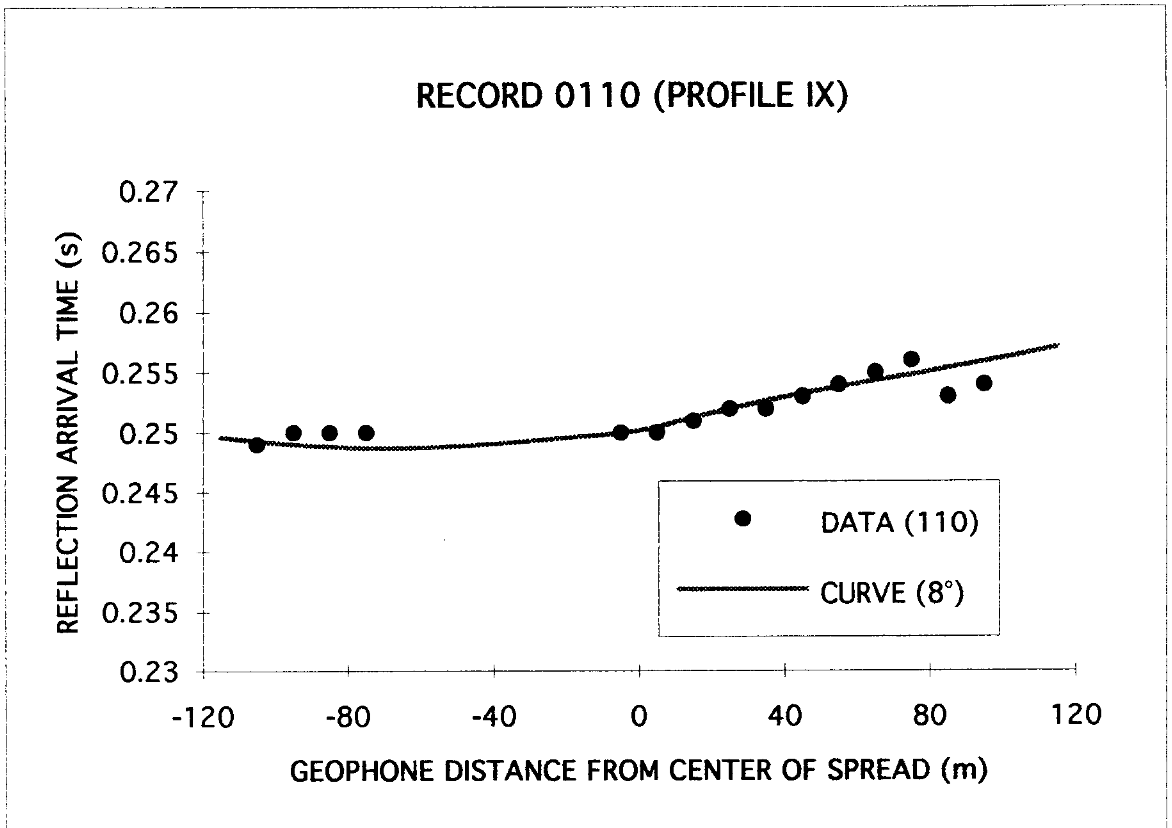
RECORD 0110 (PROFILE IX)
REFLECTION ARRIVAL TIME (s)
0.27
0.265
0.26
0.255
0.25
0.245
0.24
0.235
0.23
-120
-80
-40
0
40
80
120
GEOPHONE DISTANCE FROM CENTER OF SPREAD (m)
DATA (110)
CURVE (8°)

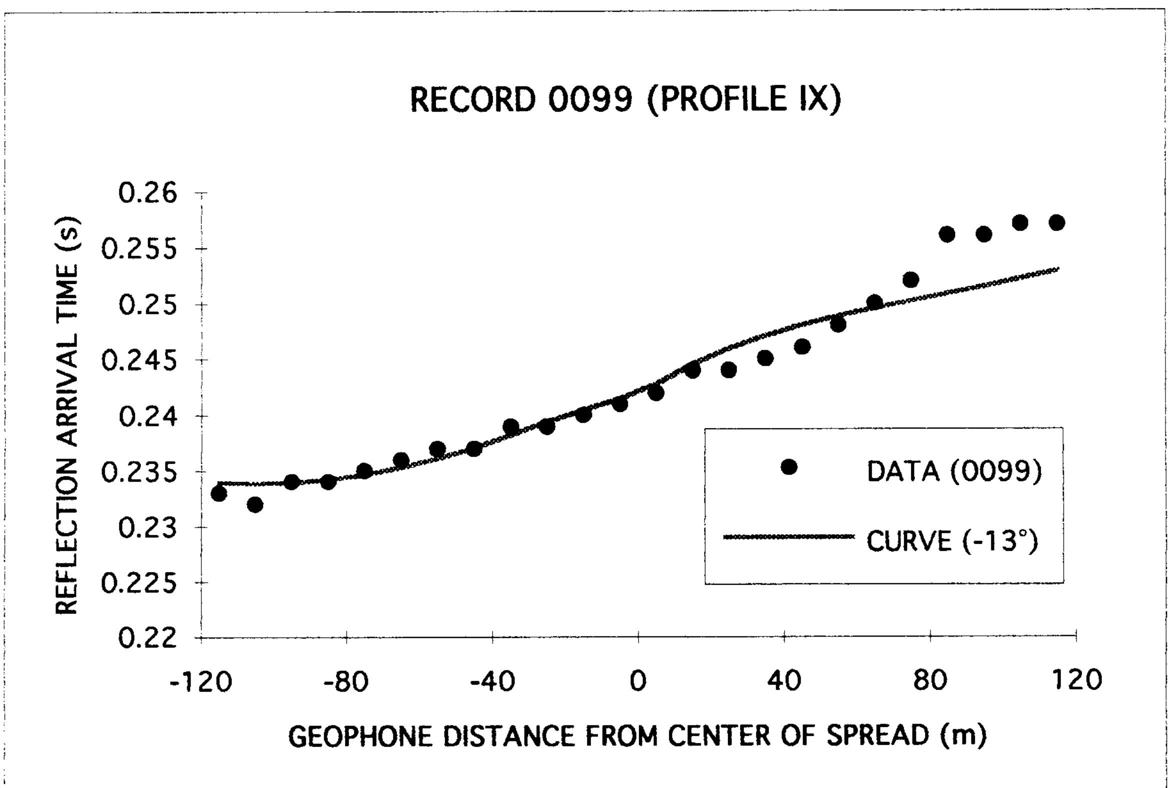
RECORD 0099 (PROFILE IX)
REFLECTION ARRIVAL TIME (s)
0.26
0.255
0.25
0.245
0.24
0.235
0.23
0.225
0.22
-120
-80
-40
0
40
80
120
GEOPHONE DISTANCE FROM CENTER OF SPREAD (m)
DATA (0099)
CURVE (-13°)

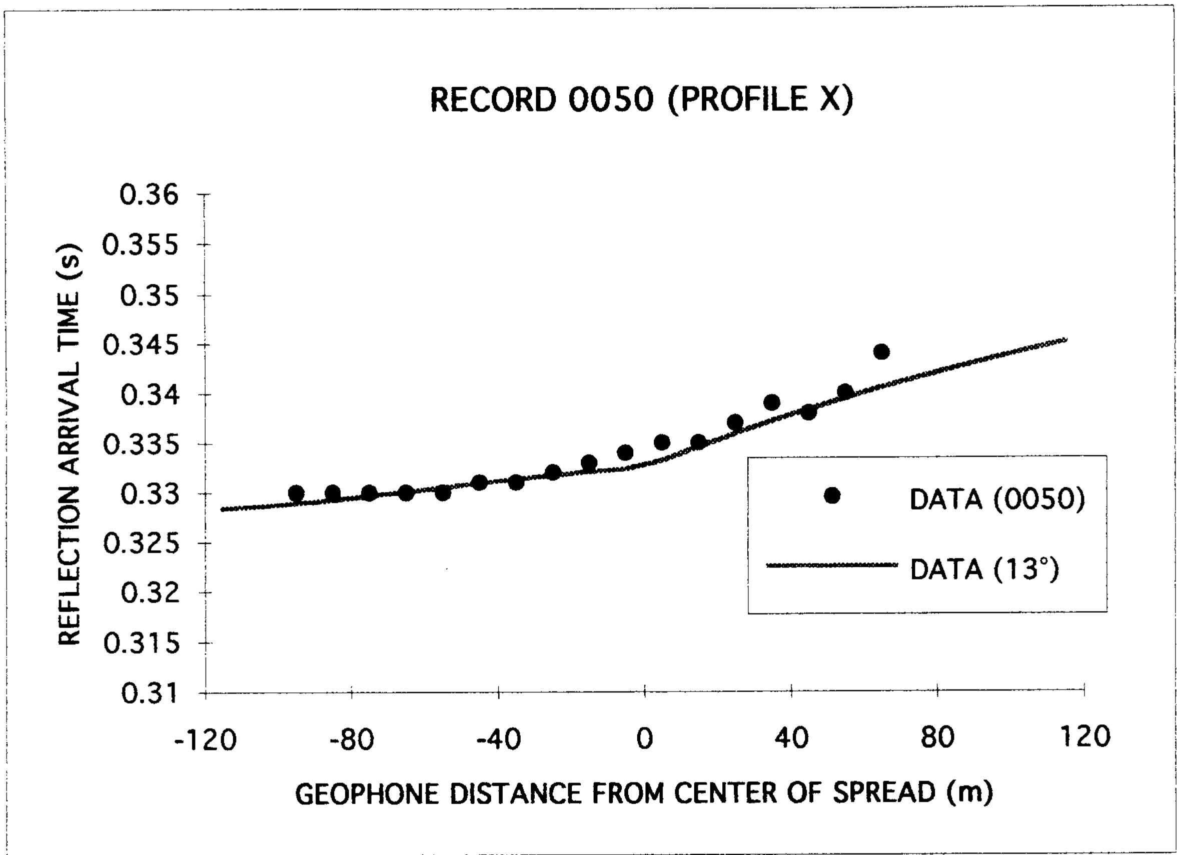
RECORD 0050 (PROFILE X)
REFLECTION ARRIVAL TIME (s)
0.36
0.355
0.35
0.345
0.34
0.335
0.33
0.325
0.32
0.315
0.31
-120
-80
-40
0
40
80
120
GEOPHONE DISTANCE FROM CENTER OF SPREAD (m)
DATA (0050)
DATA (13°)

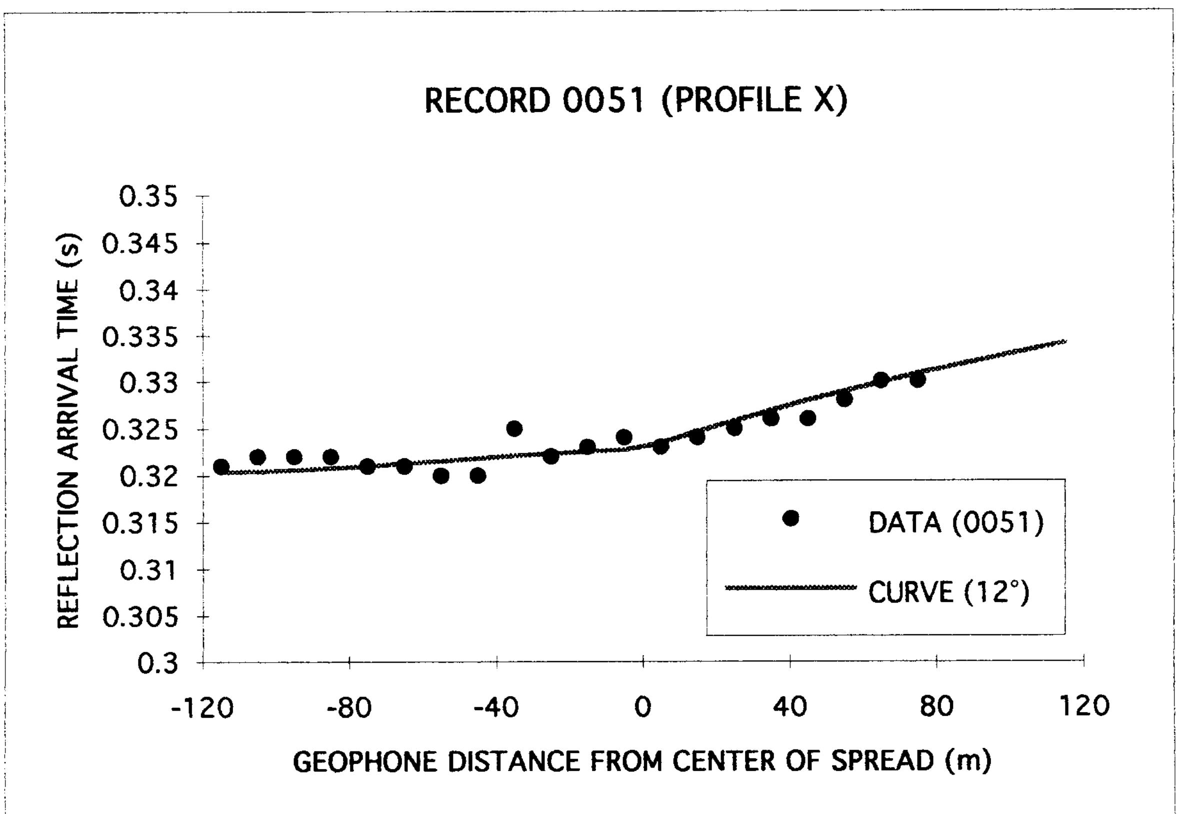
RECORD 0051 (PROFILE X)
REFLECTION ARRIVAL TIME (s)
0.35
0.345
0.34
0.335
0.33
0.325
0.32
0.315
0.31
0.305
0.3
-120
-80
-40
0
40
80
120
GEOPHONE DISTANCE FROM CENTER OF SPREAD (m)
DATA (0051)
CURVE (12°)

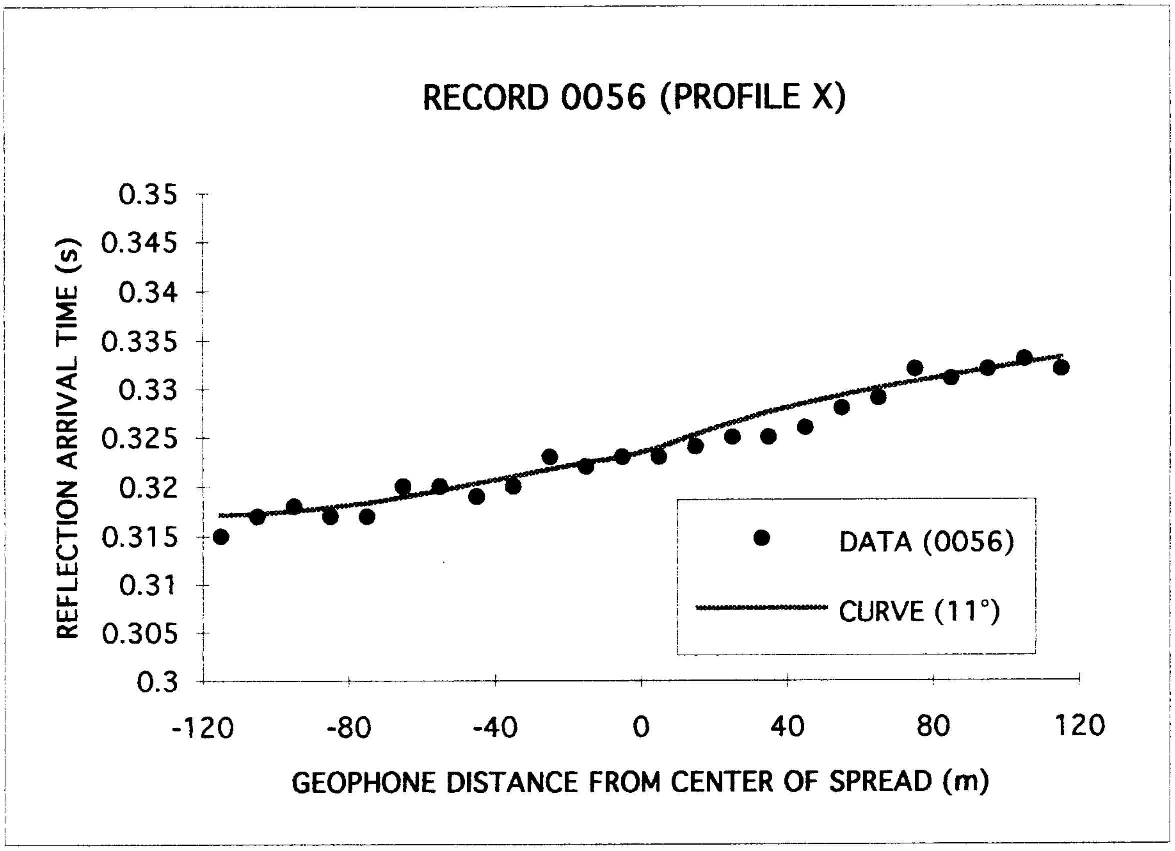
RECORD 0056 (PROFILE X)
0.35
0.345
0.34
0.335
0.33
0.325
0.32
0.315
0.31
0.305
0.3
REFLECTION ARRIVAL TIME (s)
-120
-80
-40
0
40
80
120
GEOPHONE DISTANCE FROM CENTER OF SPREAD (m)
DATA (0056)
CURVE (11°)

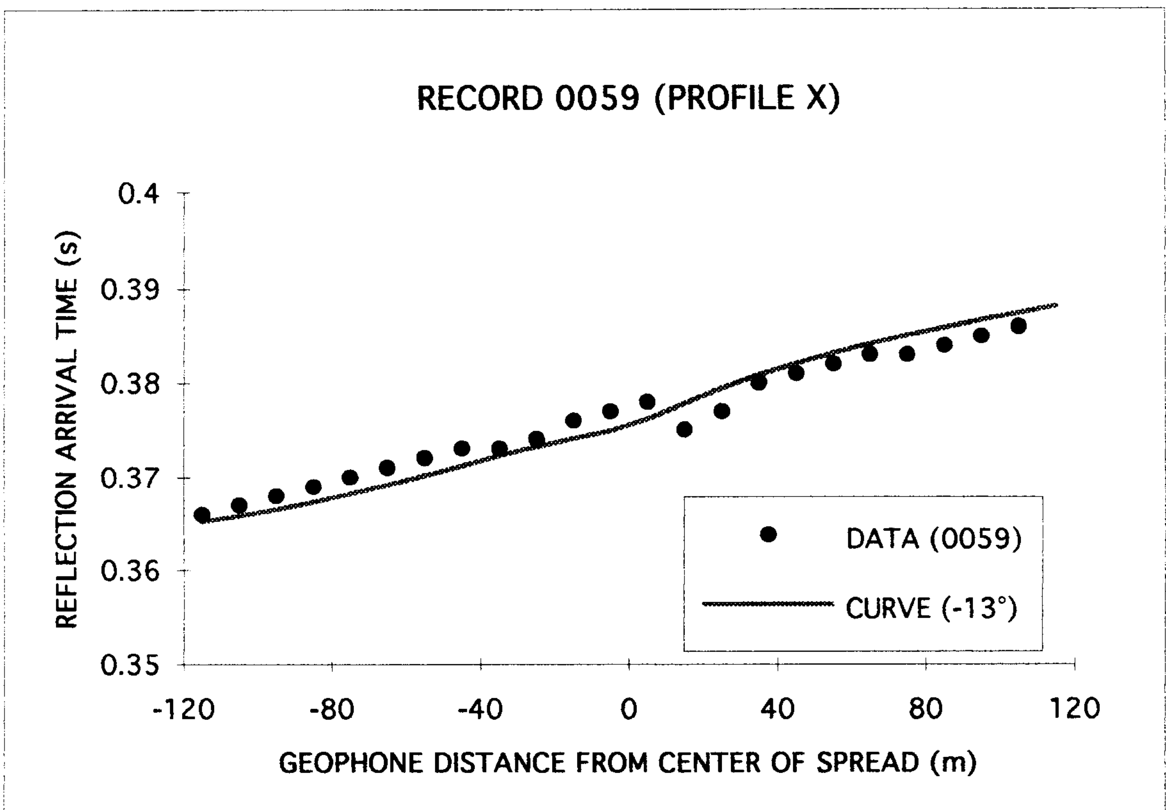
RECORD 0059 (PROFILE X)
0.4
0.39
0.38
0.37
0.36
0.35
REFLECTION ARRIVAL TIME (s)
-120
-80
-40
0
40
80
120
GEOPHONE DISTANCE FROM CENTER OF SPREAD (m)
DATA (0059)
CURVE (-13°)

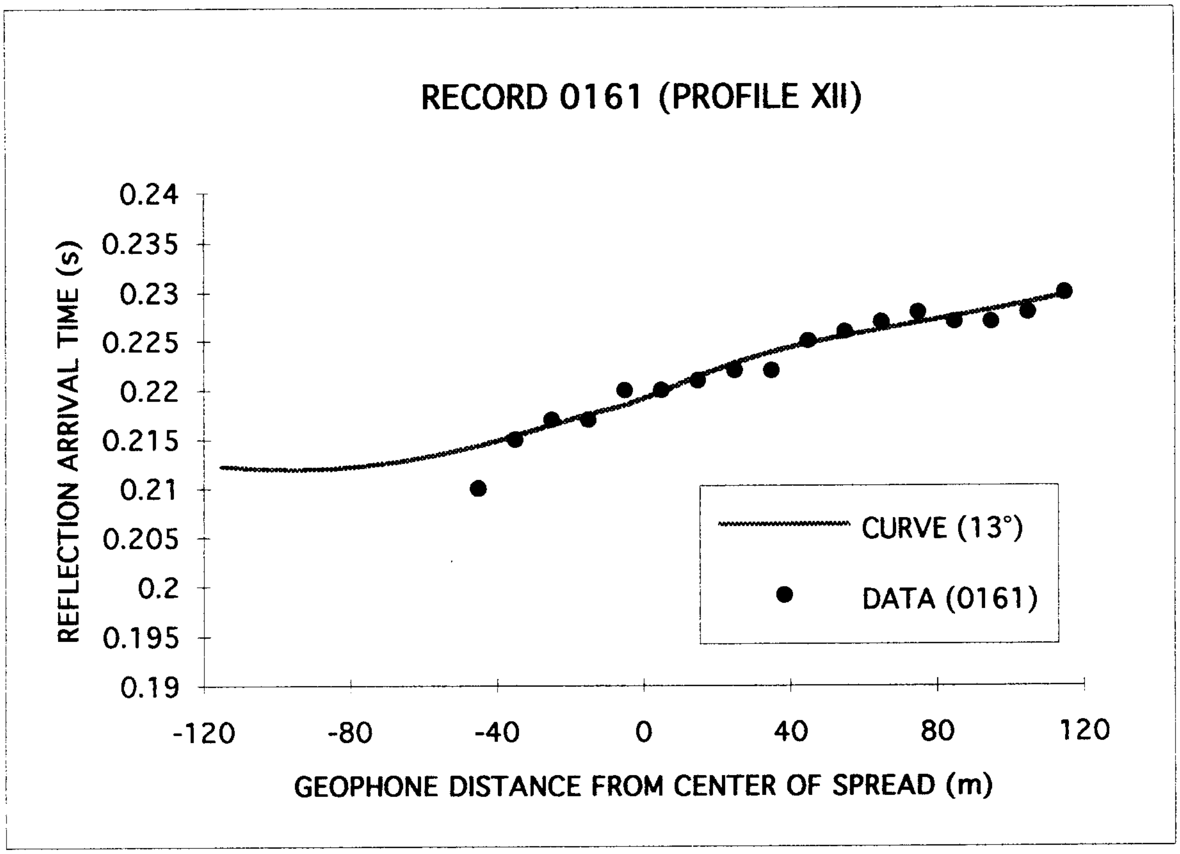

RECORD 0161 (PROFILE XII)
REFLECTION ARRIVAL TIME (s)
0.24
0.235
0.23
0.225
0.22
0.215
0.21
0.205
0.2
0.195
0.19
-120
-80
-40
0
40
80
120
GEOPHONE DISTANCE FROM CENTER OF SPREAD (m)
CURVE (13°)
DATA (0161)

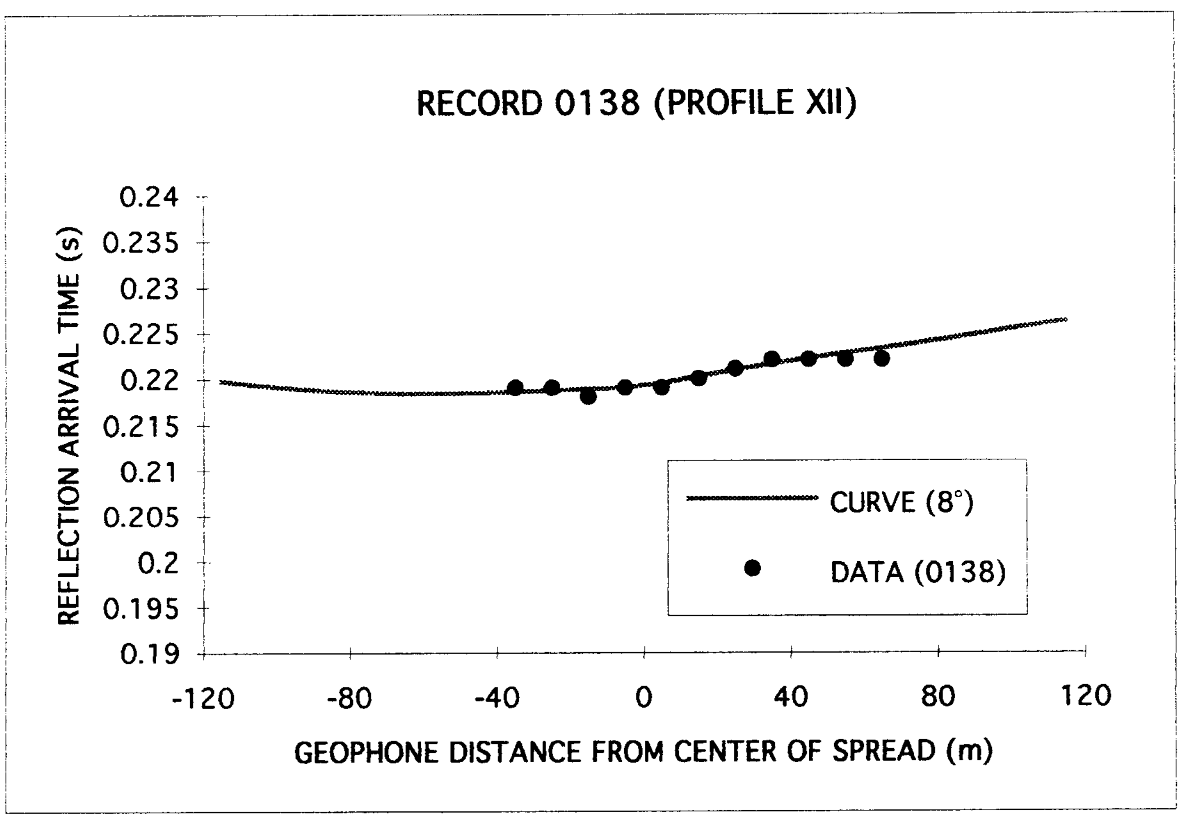

RECORD 0138 (PROFILE XII)
REFLECTION ARRIVAL TIME (s)
0.24
0.235
0.23
0.225
0.22
0.215
0.21
0.205
0.2
0.195
0.19
-120
-80
-40
0
40
80
120
GEOPHONE DISTANCE FROM CENTER OF SPREAD (m)
CURVE (8°)
DATA (0138)

References

Allen , C. R., and Smith, G. I., (1953) Seismic and gravity investigations on the Malaspina Glacier, Alaska. Transactions, American Geophysical Union, Vol. 34, No. 5, pp. 755-760.

Brockamp and Mothes, (1930) Seismic investigations on the Pasterze Glacier, Zeitschrift für Geophysik, Vol. 9, p. 482.

Doell, R. R., (1963) Seismic depth study of the Salmon Glacier, British Columbia. Journal of Glaciology, Vol. 4, No. 34, pp. 425-437.

Goldthwait, R. P., (1936) Seismic soundings on the South Crillon and Klooch Glacier,Geographical Journal, Vol. 87, pp. 496-511.

Hobson, G D., and Jobin, C., (1975) A seismic investigation - Peyto Glacier, Banff National Park and Woolsey Glacier, Mount Revelstoke National Park, Geoexploration, Vol. 13, pp. 117-127.

Kohnen, H., (1974) The temperature dependence of seismic waves in ice, Journal of Glaciology, Vol. 13, No. 67, pp. 144-147.

Marston, R. A. (1983) Supraglacial stream dynamics on the Juneau Icefield, Annals of the Association of American Geographers, No. 73, pp. 597-608.

Miller, M. M., (1985) Recent climatic variations, their causes and Neogene perspectives, in Late Cenozoic History of the Pacific Northwest, American Association for the Advancement of Science, Pacific Division; San Francisco, California, pp. 357-414.

Nolan. M., (1992) JIRP Open File Report 1992. Juneau Icefield Research Project,Foundation for Glacier and Environmental Research.

Paterson, W. S. B., (1981) The Physics of Glaciers. Pergammon Press, New York, 385 pp.

Peterson, R. A., (1949) Seismograph Air Shooting Tests, Naval Petroleum Reserve No. 4, August 1948, United Geophysical Co. Inc. Report, September 29, 1949.

Poulter, T. C., Allen, C. F., and Miller, S. W., (1950a) Seismic measurements on the Taku Glacier, in Geophysical Studies in the Antarctic; Contract N8 onr 526, ProjectNo. NR-081-020, published by the Stanford Research Institute.

Poulter, T. C. (1950b) The Poulter seismic method of geophysical exploration, Geophysics, Vol. 15, pp. 181-207.

Poulter, T. C., (1950c) The Poulter Seismic Method, The Canadian Mining and Metallurgical Bulletin, May, pp. 258-267.

Robin, G. de Q., (1953) Summary of seismic shooting investigations in Dronning Maud Land, Journal of Glaciology, Vol. 2, No. 13, pp. 205-212.

Röthlisberger, H., (1955) Studies in glacier physics on the Penny Ice Cap,Baffin Island, 1953, Part III Seismic Sounding, Journal of Glaciology, Vol. 2, No. 18, pp. 539-547.

Senstad and Rifkind, (1983) 1983 Geophysical Depth Measurements using Seismic Reflections, Juneau Icefield, Alaska. JIRP Open File Report 1983. Juneau Icefield Research Project, Foundation for Glacier and Environmental Research.